



Article

Synthesis, Computational Analysis, and Antiproliferative Activity of Novel Benzimidazole Acrylonitriles as Tubulin Polymerization Inhibitors: Part 2

Anja Beč^{1,†}, Lucija Hok^{2,†}, Leentje Persoons³, Els Vanstreels³, Dirk Daelemans³, Robert Vianello^{2,*} and Marijana Hranjec^{1,*}

¹ Department of Organic Chemistry, Faculty of Chemical Engineering and Technology, University of Zagreb, Marulićev trg 19, HR-10000 Zagreb, Croatia; abec@fkit.hr

² Laboratory for the Computational Design and Synthesis of Functional Materials, Division of Organic Chemistry and Biochemistry, Ruđer Bošković Institute, Bijenička cesta 54, HR-10000 Zagreb, Croatia; lucija.hok@irb.hr

³ KU Leuven, Department of Microbiology, Immunology and Transplantation, Laboratory of Virology and Chemotherapy, Rega Institute, 3000 Leuven, Belgium; leentje.persoons@kuleuven.be (L.P.); els.vanstreels@kuleuven.be (E.V.); dirk.daelemans@kuleuven.be (D.D.)

* Correspondence: robert.vianello@irb.hr (R.V.); mhranjec@fkit.hr (M.H.)

† These authors contributed equally to this work.

Abstract: We used classical linear and microwave-assisted synthesis methods to prepare novel *N*-substituted, benzimidazole-derived acrylonitriles with antiproliferative activity against several cancer cells in vitro. The most potent systems showed pronounced activity against all tested hematological cancer cell lines, with favorable selectivity towards normal cells. The selection of lead compounds was also tested in vitro for tubulin polymerization inhibition as a possible mechanism of biological action. A combination of docking and molecular dynamics simulations confirmed the suitability of the employed organic skeleton for the design of antitumor drugs and demonstrated that their biological activity relies on binding to the colchicine binding site in tubulin. In addition, it also underlined that higher tubulin affinities are linked with (i) bulkier alkyl and aryl moieties on the benzimidazole nitrogen and (ii) electron-donating substituents on the phenyl group that allow deeper entrance into the hydrophobic pocket within the tubulin's β -subunit, consisting of Leu255, Leu248, Met259, Ala354, and Ile378 residues.

Keywords: acrylonitriles; antiproliferative activity; benzimidazoles; docking analysis; molecular dynamics simulations; tubulin polymerization



Citation: Beč, A.; Hok, L.; Persoons, L.; Vanstreels, E.; Daelemans, D.; Vianello, R.; Hranjec, M. Synthesis, Computational Analysis, and Antiproliferative Activity of Novel Benzimidazole Acrylonitriles as Tubulin Polymerization Inhibitors: Part 2. *Pharmaceuticals* **2021**, *14*, 1052. <https://doi.org/10.3390/ph14101052>

Academic Editor: Mary J. Meegan

Received: 6 September 2021

Accepted: 13 October 2021

Published: 17 October 2021

Publisher's Note: MDPI stays neutral with regard to jurisdictional claims in published maps and institutional affiliations.



Copyright: © 2021 by the authors. Licensee MDPI, Basel, Switzerland. This article is an open access article distributed under the terms and conditions of the Creative Commons Attribution (CC BY) license (<https://creativecommons.org/licenses/by/4.0/>).

1. Introduction

Microtubules, being key dynamic structural components in cells, have attracted considerable attention from medicinal chemists as targets for anticancer drug discovery [1–3]. These protein biopolymers, formed through the polymerization of heterodimers of α - and β -tubulins, play an important role in cellular shape organization, cell division, mitosis, and intracellular movement. Potent microtubule-targeting drugs such as paclitaxel, vinblastine, colchicine, and vincristine are structurally complex natural products that are widely used in anticancer therapy [4]. These products alter the dynamics of tubulin, such as the polymerization and depolymerization [5], by binding to specific sites on the tubulin heterodimers [6], of which the most important are those for paclitaxel, vinblastine, and colchicine; thus, within the binding to the tubulin heterodimers, inhibitors could suppress tubulin dynamic instability and interfere with microtubule functions, including the mitotic spindle formation.

Inhibitors that bind to the vinblastine and colchicine binding sites are known as inhibitors of tubulin polymerization, while inhibitors interacting with the paclitaxel binding site are known as microtubule-stabilizing compounds [7].

During the past decades, there has been an increase in the development of novel tubulin polymerization inhibitors, while versatile classes of organic derivatives, both natural and synthetic, have been extensively studied [8–12]. Nowadays, considerable interest is focused on the development, design, and biological activity of novel heteroaromatic systems, whereby nitrogen heterocycles have become the essential structural motifs in medicinal and pharmaceutical chemistry, being very important in drug discovery. Benzimidazoles can easily interact with essential biomolecules of living systems due to the structural similarity of their nuclei with naturally occurring purines. Benzimidazoles are, therefore, very prominent scaffolds for the development of novel derivatives with a wide range of diverse biological activities. Considering all of the biological activities displayed by benzimidazoles, one of the most important is their antitumor activity, which is exerted by acting on numerous biological targets (Figure 1). For example, they can interact with DNA and RNA as intercalators or minor groove binders [13]; they can inhibit topoisomerases I and II [14]; and they can act as antiangiogenic agents [15], androgen receptor antagonists [16], and inhibitors of kinases [17,18]. Some benzimidazoles were also recognized as tubulin polymerization inhibitors, mostly binding to the colchicine binding site [19–22]. Nocodazole (Figure 1a) is a well-known anticancer agent, which significantly inhibits tubulin polymerization at low nanomolar concentrations [23]. Additionally, benzimidazole-5-carboxylate derivatives causes mitotic catastrophes by specifically targeting the microtubule system [24]. Several studies have reported on the biological activity of 2-aryl-1,2,4-oxadiazolo-benzimidazole derivatives (Figure 1b) with different mechanisms of biological action, such as binding to the colchicine binding site [25]. A series of benzimidazole-2-urea derivatives (Figure 1c) has been described as novel β -tubulin inhibitors that might bind in a new binding site different from the three well-known ones [26]. Novel 2-aryl-benzimidazole derivatives of dehydroabietic acid have been reported as tubulin polymerization inhibitors, which significantly disrupt the intracellular microtubule network by binding to the colchicine site of tubulin [26].

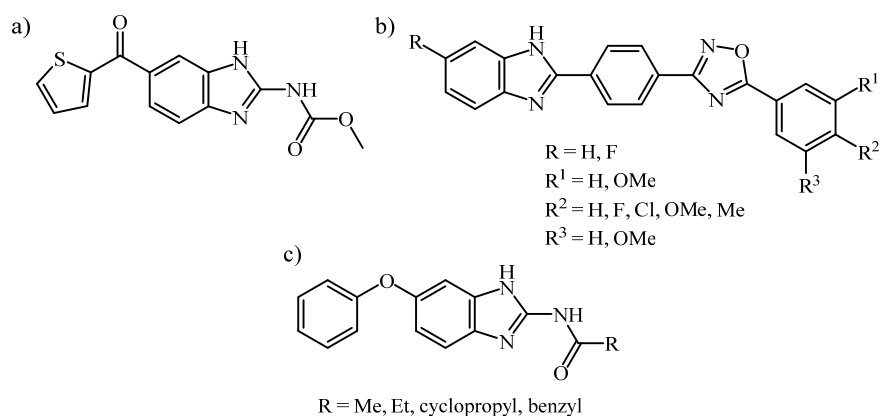


Figure 1. Benzimidazole-derived tubulin polymerization inhibitors: (a) Nocodazole; (b) 2-aryl-1,2,4-oxadiazolo-benzimidazole derivatives; (c) benzimidazole-2-urea derivatives.

Recently, as a continuation of our previous efforts aimed at the design and discovery of novel benzimidazoles with promising antitumor activities, we prepared novel *N*-substituted, benzimidazole-derived acrylonitriles as potential tubulin polymerization inhibitors. *N,N*-dimethylamino-substituted acrylonitriles **I** and **II** (Figure 2) with submicromolar inhibitory concentrations (IC_{50} 0.2–0.6 μ M) were chosen as lead compounds, while their interference with the tubulin activity was confirmed by *in vitro* studies of the tubulin polymerization inhibition and the computational analysis [27].

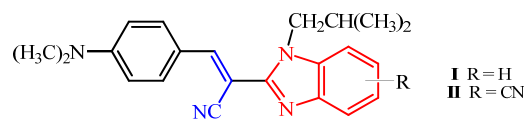


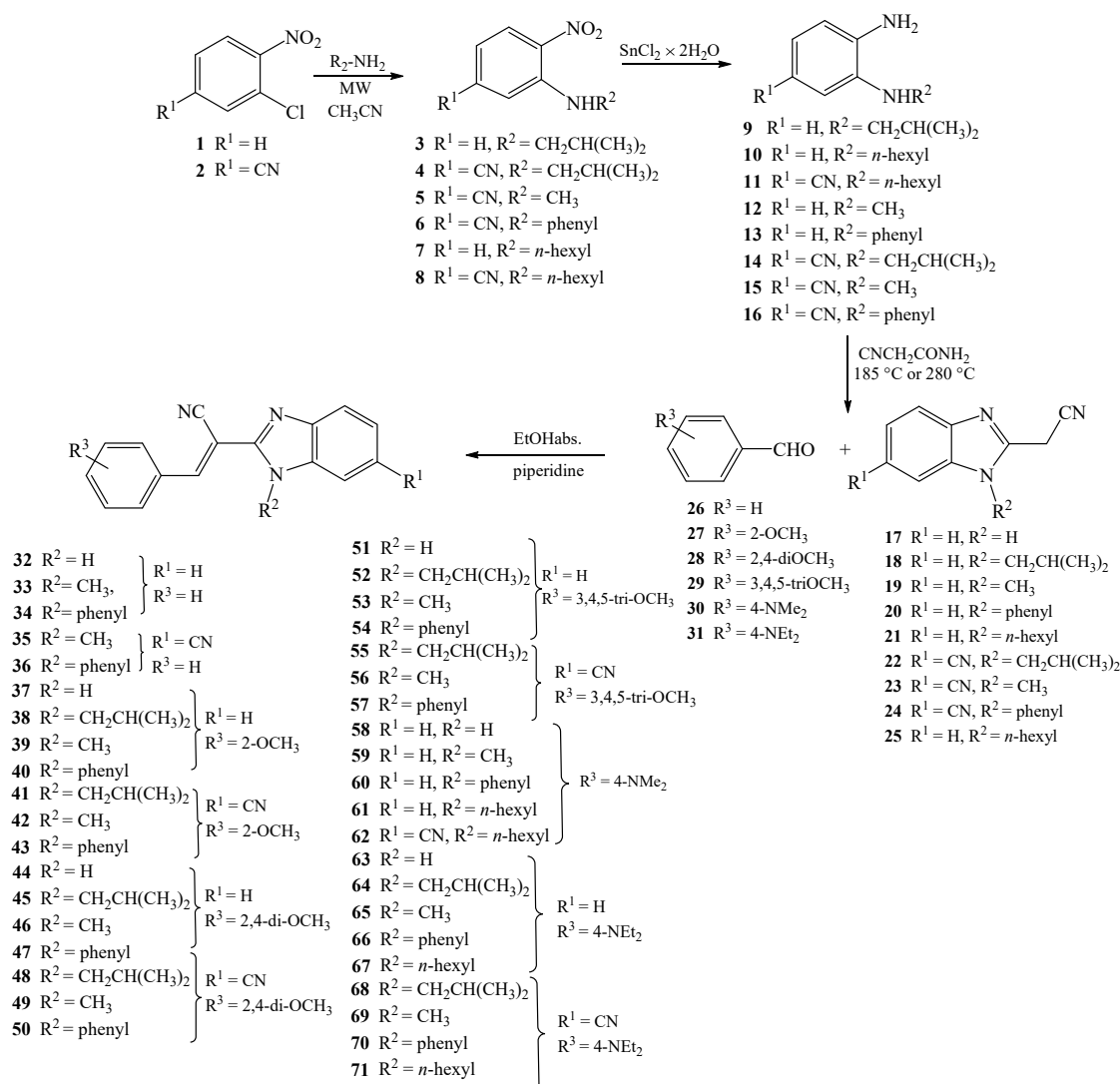
Figure 2. Benzimidazole acrylonitriles **I** and **II** as tubulin polymerization inhibitors.

Encouraged by our findings and the fact that some of the tested compounds showed strong and selective antiproliferative activity, we further optimized the presented structure by designing and synthesizing novel *N*-substituted benzimidazole acrylonitriles. Here, we present the synthesis, biological activity, and tubulin polymerization inhibition of the most active compounds and demonstrate their binding within the colchicine site of tubulin via computational docking analysis and molecular dynamics simulations.

2. Results and Discussion

2.1. Chemistry

The synthesis of novel *N*-substituted, benzimidazole-derived acrylonitriles **32–71** is illustrated in Scheme 1, starting from the *ortho*-chloronitrobenzenes **1–2**.



Scheme 1. Synthesis of benzimidazole acrylonitriles **32–71**.

By using uncatalyzed microwave-assisted amination in acetonitrile with an excess of desired amine, *N*-substituted precursors **3–8** bearing *i*-butyl, methyl, phenyl, and *n*-hexyl substituents were obtained in good reaction yields. Within the reduction of nitro-substituted compounds **3–8** with $\text{SnCl}_2 \cdot 2\text{H}_2\text{O}$ in MeOH followed by cyclocondensation with 2-cyanoacetamide at high temperatures, corresponding *N*-substituted 2-(cyanomethyl)-benzimidazoles **17–25** as main precursors were obtained in moderate yields [27]. Targeted acrylonitrile derivatives **32–71** were synthesized in the condensation with the chosen unsubstituted and methoxy-, *N,N*-dimethyl-, and *N,N*-diethyl-substituted aromatic aldehydes **26–31** in absolute ethanol by using a few drops of piperidine as a weak base. All acrylonitriles were obtained in moderate to high reaction yields, while some of them were obtained as mixtures of *E*- and *Z*-isomers (**38**, **41**, **45**, **61**, **64**, **67**, and **68**), which could not be efficiently separated by column chromatography.

The structural determination of newly prepared acrylonitriles was performed using ^1H and ^{13}C NMR spectroscopies and elemental analysis. The structural characterization was performed based on the chemical shifts in both spectra and H-H coupling constant values in the ^1H spectra. The successful nucleophilic substitution was confirmed within the signals in the aliphatic part of both ^1H and ^{13}C NMR spectra of compounds **3–8**. The structure of amino-substituted derivatives **9–16** was confirmed via the observation of signals related to the protons of amino groups placed in the range of 5.25–4.44 ppm in the ^1H NMR spectra. A singlet of acrylonitrile protons in the range of 8.54–7.20 ppm confirmed the formation of acrylonitrile derivatives.

2.2. Biological Evaluation

2.2.1. Antiproliferative Activity In Vitro

All newly prepared compounds were tested for their antiproliferative activity in vitro. The results are displayed in Table 1 as IC_{50} values (50% inhibitory concentrations) and are compared to known antiproliferative agents combretastatin A4 (CA4) and docetaxel.

For the biological evaluation, eight human cancer cells from different cancer types were used (LN-229—glioblastoma; Capan-1—pancreatic adenocarcinoma; HCT-116—colorectal carcinoma; NCI-H460—lung carcinoma; DND-41—acute lymphoblastic leukemia; HL-60—acute myeloid leukemia; K-562—chronic myeloid leukemia; Z-138—non-Hodgkin lymphoma). The majority of the compounds exerted weak to moderate antiproliferative activity on the tested cell lines, while compounds **50**, **64**, **68**, and **69** showed exceptionally strong antiproliferative activity against some, but not all, of the cancer cells.

Thirteen derivatives did not show any activity against the tested cell lines. Some of the tested derivatives exhibited strong and selective antiproliferative activity but were less active in comparison to the used standard drugs. Among the most active compounds, the *N,N*-diethylamino-substituted derivative with the *i*-butyl substituent placed at the nitrogen atom of benzimidazole core **64** did not show any significant selectivity towards the tested cancer cell lines and was the most potent system elucidated here. Compound **50** substituted with cyano and phenyl rings at the benzimidazole core bearing two methoxy groups, **68** substituted with cyano and *i*-butyl substituents at the benzimidazole core bearing a *N,N*-diethylamino group, and **69** substituted with cyano and methyl substituents at the benzimidazole core bearing a *N,N*-diethylamino group showed selectivity against the hematological cancer cell lines (acute lymphoblastic leukemia (DND-41), acute myeloid leukemia (HL-60), chronic myeloid leukemia (K-562), and non-Hodgkin lymphoma (Z-138)). Among other derivatives with moderate activities, compound **48** substituted with cyano and *i*-butyl at the benzimidazole core bearing two methoxy groups showed some selectivity against lung carcinoma (NCI-H460) and colorectal carcinoma (HCT-116).

In general, comparing the unsubstituted and cyano-substituted derivatives bearing the same substituents at the nitrogen atom of the benzimidazole core and at the phenyl ring, it was observed that some cyano-substituted derivatives showed slightly improved antiproliferative activity, while for some others the presence of the $-\text{CN}$ moiety reduced the activity.

Table 1. Antiproliferative activities of in vitro of compounds 32–69 expressed as IC₅₀ values (μM). Values are presented as the means ± SD of *n* = 2 independent experiments.

Cpd	R ¹	R ²	R ³	Cell Line									
				LN-229	Capan-1	HCT-116	NCI-H460	DND-41	HL-60	K-562	Z-138		
32	H	H	H	>100	≥87.5	>100	>100	>100	>100	>100	>100	>100	13.7 ± 2.7
33	H	Me	H	>100	≥64.1	>100	>100	>100	>100	≥39.1	≥74.2	>100	>100
35	CN	Me	H	>100	>100	>100	>100	>100	>100	≥79.0	>100	>100	>100
38	H	<i>i</i> -Bu	2-OMe	>100	>100	≥51.6	>100	>100	>100	≥48.0	≥74.8	>100	>100
39	H	Me	2-OMe	>100	>100	>100	>100	>100	>100	≥46.4	≥42.8	>100	>100
40	H	Ph	2-OMe	>100	>100	>100	>100	>100	>100	>100	38.4 ± 35.1	>100	>100
41	CN	<i>i</i> -Bu	2-OMe	>100	≥49.3	≥56.1	>100	>100	>100	≥81.7	>100	>100	>100
42	CN	Me	2-OMe	>100	≥52.0	>100	>100	>100	>100	>100	>100	>100	>100
43	CN	Ph	2-OMe	>100	>100	>100	>100	>100	>100	≥83.5	>100	>100	>100
44	H	H	2,4-(OMe) ₂	≥99.3	≥38.4	>100	>100	>100	>100	>100	73.5 ± 10.6	>100	>100
45	H	<i>i</i> -Bu	2,4-(OMe) ₂	≥48.3	≥51.9	32.9 ± 30.3	>100	>100	>100	≥32.7	≥59.1	≥46.9	>100
46	H	Me	2,4-(OMe) ₂	>100	>100	>100	>100	>100	>100	≥99.7	>100	>100	>100
47	H	Ph	2,4-(OMe) ₂	>100	57.0 ± 9.2	≥56.5	>100	>100	>100	≥29.8	≥66.6	>100	>100
48	CN	<i>i</i> -Bu	2,4-(OMe) ₂	44.0 ± 33.9	21.7 ± 4.2	14.0 ± 1.4	18.2 ± 6.1	36.4 ± 2.6	28.3 ± 15.1	≥44.9	≥44.9	27.7 ± 16.5	>100
50	CN	Ph	2,4-(OMe) ₂	>100	56.3 ± 12.2	≥61.3	≥93.8	1.7 ± 1.7	2.1 ± 0.4	3.3 ± 0.1	2.8 ± 0.1	>100	>100
51	H	H	3,4,5-(OMe) ₃	>100	≥85.6	>100	>100	>100	>100	≥35.2	≥40.0	>100	>100
52	H	<i>i</i> -Bu	3,4,5-(OMe) ₃	≥71.3	≥46.5	≥49.0	>100	>100	>100	47.2 ± 26.1	>100	≥45.9	>100
53	H	Me	3,4,5-(OMe) ₃	>100	≥52.7	>100	>100	>100	>100	≥59.7	>100	>100	>100
54	H	Ph	3,4,5-(OMe) ₃	>100	>100	≥67.6	>100	>100	62.6 ± 17.7	43.4 ± 37.5	>100	50.7 ± 4.5	>100
59	H	Me	4-NMe ₂	>100	>100	>100	>100	>100	>100	≥49.4	>100	≥53.1	>100
61	H	<i>n</i> -Hx	4-NMe ₂	>100	≥61.2	≥57.7	>100	>100	>100	40.4 ± 6.6	≥88.2	>100	>100
64	H	<i>i</i> -Bu	4-NEt ₂	3.0 ± 1.6	2.0 ± 0.1	1.8 ± 0.9	2.9 ± 0.5	2.8 ± 1.1	3.6 ± 2.3	2.5 ± 0.6	2.5 ± 0.6	5.9 ± 2.3	>100
65	H	Me	4-NEt ₂	≥97.8	≥37.3	>100	>100	>100	50.0 ± 0.9	42.8 ± 4.9	44.3 ± 33.8	46.6 ± 0.1	>100
66	H	Ph	4-NEt ₂	>100	≥99.2	>100	>100	>100	>100	>100	>100	>100	>100
68	CN	<i>i</i> -Bu	4-NEt ₂	72.5 ± 3.3	29.9 ± 26.7	54.0 ± 0.9	66.9 ± 9.5	1.6 ± 0.3	2.5 ± 1.1	2.4 ± 1.4	2.4 ± 1.4	1.4 ± 0.7	>100
69	CN	Me	4-NEt ₂	>100	59.3 ± 0.8	≥83.8	>100	>100	2.2 ± 1.8	2.7 ± 1.1	2.9 ± 1.5	3.4 ± 0.8	>100
		Docetaxel		0.0030 ± 0.0001	0.0412 ± 0.0029	0.0022 ± 0.0000	0.0024 ± 0.0006	0.0027 ± 0.0001	0.0017 ± 0.0002	0.0562 ± 0.032	0.0019 ± 0.0001	0.0019 ± 0.0001	>100
		CA4		0.0003 ± 0.0001	0.0003 ± 0.0002	0.0015 ± 0.0009	0.0041 ± 0.0003	0.0011 ± 0.0001	0.0008 ± 0.0001	0.0011 ± 0.0010	0.0004 ± 0.0002	0.0004 ± 0.0002	>100

The latter also holds for the most potent compound **64**, whose cyano derivative **68** is generally less active. Among the tested systems, *i*-butyl-substituted derivatives showed improved activity relative to methyl, phenyl or *n*-hexyl-substituted analogues. According to the obtained results, it is obvious that the most significant impact on the antiproliferative activity enhancement relates to the introduction of the *N,N*-diethylamino group at the *para*-position of the phenyl ring. In comparison to the previously published results [27], it can be concluded that the introduction of the *N,N*-diethylamino group instead of the *N,N*-dimethylamino group decreased the antiproliferative activity against Capan-1, HCT-116, NCI-H460, DND-41, and HL-60 cancer cells from a submicromolar to micromolar range of inhibitory concentrations.

In order to establish whether the observed antiproliferative activity is selective towards cancer cells, normal peripheral blood mononuclear cells (PBMCs) from two healthy donors were treated with compounds **50**, **64**, **68**, and **69** (Figure 3). The compounds with the best antiproliferative activity in hematological cancer cells (compound **50**, **68**, and **69**) also induced apoptosis in normal cells, although this was limited to the highest concentration tested (20 μ M) for compounds **68** and **69**, resulting in a favorable selectivity window. Derivative **64**, which was inhibitory against all tested cancer cell lines, had no effect on the viability of normal PBMC and is, thus, a selective anticancer compound.

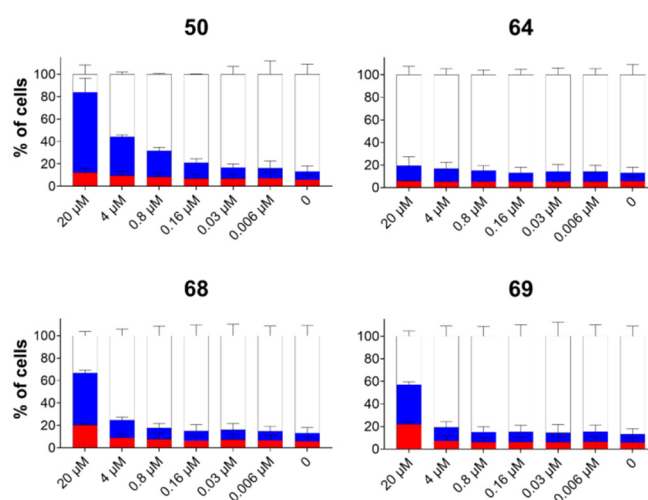


Figure 3. Effects of derivatives **50**, **64**, **68**, and **69** on normal PBMC. Apoptosis induction in PBMC from two healthy donors was determined by staining with IncuCyte[®] Caspase 3/7 Green Reagent and PI followed by live cell monitoring. The percentages of live (white), dead (red), and apoptotic (blue) cells after 72 h are shown (means \pm standard error bars).

2.2.2. In Vitro Inhibition of the Tubulin Polymerization

The ability of derivatives **50**, **64**, **68**, and **69** to inhibit the polymerization of tubulin was confirmed in vitro in a purified protein system. All tested compounds showed effective activity in a dose-dependent manner (Figure 4).

At the highest concentrations tested (30 and 10 μ M), these four derivatives were all able to inhibit tubulin polymerization. Even when lowering the dose to 3 μ M, compounds **50** (to a lesser extent) and **68** still showed some inhibitory activity in the in vitro assay.

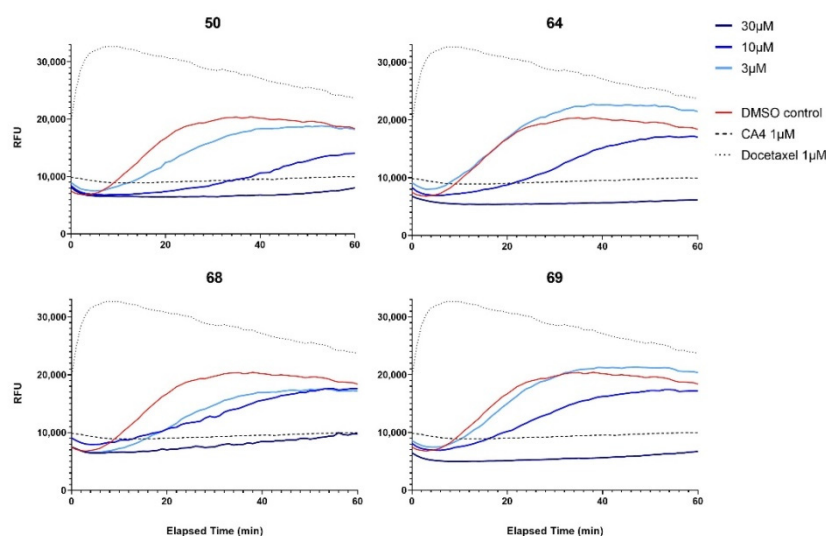


Figure 4. Dose-dependent effects of compounds **50**, **64**, **68**, and **69** on in vitro tubulin polymerization. Purified porcine neuronal tubulin and GTP were mixed in a 96-well plate. Docetaxel and combretastatin A4 (CA4) ($1 \mu\text{M}$) were used as controls for tubulin-stabilizing and tubulin-destabilizing agents, respectively, while DMSO was used as a negative control. The effects on tubulin assembly were monitored in a Tecan Spark multimode plate reader at one minute intervals for one hour at 37°C . Each condition was tested in duplicate. The level of polymerization was measured by an increase in fluorescence emission intensity at $\lambda_{\text{em}} = 435 \text{ nm}$.

2.3. Computational Analysis

Computational analysis was performed to interpret the observed biological properties and to identify structural and electronic features responsible for the highest activity of **64**, which should aid in the subsequent design of even more effective ligands based on the utilized organic skeleton. To do so, we considered a representative set of compounds, including **50**, **63**, **64**, **66**, **68**, and **69**, together with two model systems **m1** and **m2**, as well as colchicine, which was taken as a typical ligand for the colchicine binding site in tubulin (Figure 5), in line with our previous results [27].

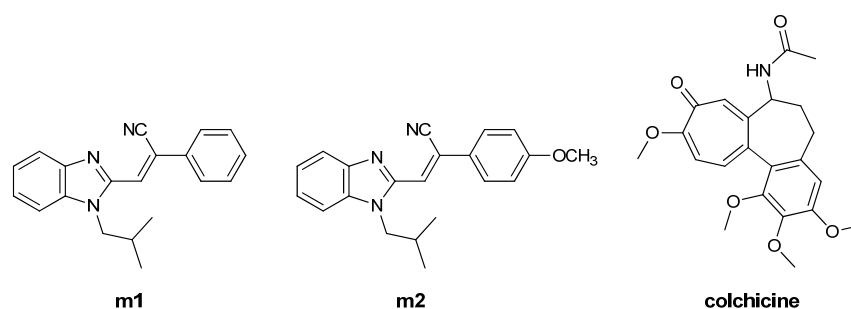


Figure 5. Chemical structures of reference systems **m1**, **m2**, and colchicine, as discussed in the text.

The systems investigated here consisted of variously substituted benzimidazole and phenyl fragments, linked together with an acrylonitrile unit, which can formally exist as either *E*- or *Z*-isomers. Our DFT analysis showed that all systems were between 0.5 and $4.0 \text{ kcal mol}^{-1}$ more stable as *Z*-isomers (Table 2 and Figure S120), where the cyano group and the benzimidazole moiety reside on the same side of the $\text{C}=\text{C}$ double bond. Although these values neglected any kinetic aspects of the isomer formation, the obtained thermodynamic data were found to be in good quantitative agreement with the experiments, which generally predict the predominance of *Z*-isomers. The differences in the stability among isomers were higher for the systems with bulkier *N*-substituents due to

larger unfavorable steric interactions with the attached phenyl group occurring in their *E*-analogues. Interestingly, the only exception was provided by the most active system, **64**, which was 1.2 kcal mol⁻¹ more stable as an *E*-analogue. This confirms its experimentally observed preference for the *E*-isomer at a 2:1 ratio, yet such the small energy difference observed here, and in other evaluated systems, allows for the presence of the other isomer as well. With this in mind, we will focus our discussion on the most stable *Z*-isomers of all systems, while both isomers will be considered for the most active compound **64**.

Table 2. Relative stability levels of the isomers, obtained using the DFT (SMD)/M06-2X/6-31+G(d) model, and the binding free energies ($\Delta G_{\text{bind,CALC}}$), obtained through docking simulations, for the studied ligands and colchicine (all values in kcal mol⁻¹). ^a The experimental value for colchicine is taken from [28].

System	Isomer	Relative Stability	$\Delta G_{\text{bind,CALC}}$	Binding Position
m1	<i>Z</i> -isomer	−2.3 from <i>E</i> -isomer	−8.0	allosteric binding
			−7.6	colchicine binding site
m2	<i>Z</i> -isomer	−1.6 from <i>E</i> -isomer	−8.4	allosteric binding
			−8.0	colchicine binding site
50	<i>Z</i> -isomer	−0.6 from <i>E</i> -isomer	−8.6	colchicine binding site
63	<i>Z</i> -isomer	−3.1 from <i>E</i> -isomer	−8.3	allosteric binding
			−8.0	colchicine binding site
64	<i>E</i> -isomer	−1.2 from <i>Z</i> -isomer	−8.7	colchicine binding site
			<i>Z</i> -isomer	+1.2 from <i>E</i> -isomer
66	<i>Z</i> -isomer	−2.9 from <i>E</i> -isomer	−8.8	allosteric binding
			−8.6	colchicine binding site
68	<i>Z</i> -isomer	−3.5 from <i>E</i> -isomer	−8.6	allosteric binding
			−8.1	colchicine binding site
69	<i>Z</i> -isomer	−4.0 from <i>E</i> -isomer	−8.3	colchicine binding site
			−9.3	colchicine binding site
colchicine	–	–	[−8.3] _{EXP} ^a	colchicine binding site

The docking procedure produced the binding free energies shown in Table 2. The highest affinity was obtained for colchicine, $\Delta G_{\text{bind}} = -9.3$ kcal mol⁻¹, closely matching the value of $\Delta G_{\text{bind}} = -9.0$ kcal mol⁻¹ reported by Silva-García and co-workers obtained using the AutoDock docking software [28]. Moreover, both of these values were in excellent agreement with the experimental value of $\Delta G_{\text{bind,EXP}} = -8.3$ kcal mol⁻¹ calculated from the colchicine binding constant $K_{\text{bind,EXP}} = 6.3 \times 10^5$ L mol⁻¹ measured by Wilson and Meza [29]. In addition, the predicted colchicine binding position very closely matched that in the crystal structure, suggesting that the docking procedure correctly positioned it within the colchicine binding site (Figure S121). Such an agreement in terms of both the binding energy and the position of the ligand leads us to conclude that these results lend firm credence to the employed computational methodology and support the reliability of the other results as well.

In certain cases, the values correspond to allosteric positions on tubulin (Figure S122), which is why we also analyzed the most favorable orthosteric poses within the colchicine binding site, since the latter are responsible for a potential tubulin polymerization inhibition. The lowest binding affinity was displayed by the least substituted **m1**, $\Delta G_{\text{bind}} = -8.0$ kcal mol⁻¹, corresponding to the allosteric binding, which suggests a lack of antitumor activity. This already suggests that the substitution of the used organic framework is likely crucial for the binding and that specific protein–ligand interactions govern the activity. Since **m1** is a reference system, let us note that a binding pose within the colchicine binding site comes with a further lower affinity, $\Delta G_{\text{bind}} = -7.6$ kcal mol⁻¹, being the least exergonic site here. In that case (Figure S123), **m1** is oriented so that its phenyl unit is immersed into the β -subunit close to Cys241, but without any significant interaction with it. In contrast, the importance of the benzimidazole unit is seen in favorable N–H $\cdots\pi$ interactions with Lys352, yet this is outperformed by the unfavorable steric contacts between *N*-*i*-butyl,

Lys254, and Asn258, which decrease the binding and disfavor such orthosteric positions for **m1**.

The addition of electron donors on the phenyl unit, such as the *p*-OMe group in **m2**, improves the binding. This allows deeper penetration of the β -subunit (Figure S123) facilitated by the S–H \cdots O(Me) hydrogen bonding with Cys241, which is absent in **m1**. This maintains favorable contacts with Lys352, while offering reduced steric interactions with Lys254 and Asn258, with the latter being allowed to engage in N–H \cdots N hydrogen bonds with the benzimidazole moiety. All of this contributes around 0.4 kcal mol^{−1} to the binding within the colchicine binding site, yet still promotes the allosteric binding as being the most favorable at $\Delta G_{\text{bind}} = -8.4$ kcal mol^{−1}. Replacing the *p*-OMe group with *p*-NEt₂ immediately offers the most potent system **64**. With its better hydrogen-bond-accepting properties, **64** forms a stronger S–H \cdots N(Et₂) interaction with Cys241 (Figure S123), which is evident in the reduced S \cdots N distance of 0.4 Å from that observed for the matching S \cdots O distance in **m2**. This allows **64** to rotate and avoid the unfavorable steric contacts with Lys254 and Asn258, enabling both to bind the benzimidazole fragment—the former through the N–H \cdots π interactions, while the latter through the N–H \cdots N hydrogen bonds. The attached cyano group in **64** accepts hydrogen bonding from Lys352, further promoting the binding.

All of this positions **64** within the colchicine binding site as the most favorable binding location, linked with the most exergonic binding energy of $\Delta G_{\text{bind}} = -8.7$ kcal mol^{−1}. This confirms its high activity and promotes the tubulin polymerization inhibition as its likely biological mechanism of action.

The presence of the bulky *N*-*i*-butyl group is also significant in this activity. In general, this allows the investigated ligands to better position themselves within the hydrophobic interior of the β -subunit. If this is replaced by a smaller *N*-Me group as in **63**, the system is reverted back to the allosteric binding as being most favorable, confirming its reduced activity, while its potential binding within the colchicine binding is also reduced to $\Delta G_{\text{bind}} = -8.0$ kcal mol^{−1} (Figure S124). Along these lines, the introduction of the aromatic *N*-phenyl unit in **66** improves the binding within the colchicine binding site to $\Delta G_{\text{bind}} = -8.6$ kcal mol^{−1}, mostly through favorable N–H \cdots π interactions with this substituent, while positive contributions from Lys254 remain limited, yet this binding pose is also dominated by the allosteric binding that is 0.2 kcal mol^{−1} higher, making **66** a non-active compound.

Lastly, the presence of the electron-withdrawing cyano group on the benzimidazole core generally leads to reduced activities in the investigated cases. As illustrative examples, both **68** and **69** are associated with lower affinities than **64**, regardless of having either *N*-*i*-butyl or *N*-methyl groups attached to the benzimidazole unit. In **68**, this results in promoting the allosteric binding and allowing for only a moderate orthosteric binding at $\Delta G_{\text{bind}} = -8.1$ kcal mol^{−1}, while in **69** the effect is smaller, although seen in reduced orthosteric binding at $\Delta G_{\text{bind}} = -8.3$ kcal mol^{−1} due to a notable departure from the β -subunit interior (Figure S124). In both cases, the reduced affinity likely comes as a result of a depleted electron density within the benzimidazole unit, which makes it less susceptible for the N–H \cdots π interactions with either Lys254 or Lys352 residues and favors ligand departure from the colchicine binding site.

The results presented so far confirm **64** as the most potent ligand and reveal its position within the colchicine binding site as the most favorable binding location. Knowing that it was isolated as a mixture of both isomers, we decided to further support its prevalence for the *E*-isomer and its likely biological activity through a series of MD simulations considering both isomers. It turned out that when a less stable *Z*-isomer is placed within the colchicine binding site, it leaves this location after 130 ns of the simulation time, only to remain allosterically bound for the rest of the simulations (Figure S125). The MM-GBSA analysis reveals that during the first part of the simulation, while orthostericly bound, its binding free energy is 2.1 kcal mol^{−1} lower than during the second part, when it is positioned outside the colchicine binding site, thereby providing the driving force for the

departure (Figure S126). On the other hand, its *E*-isomer remains within the colchicine binding site throughout the MD simulations (Figure S127), while the decomposition of the obtained binding energy into contributions from individual residues demonstrates interesting trends (Figure 6). This confirms the hydrophobic nature of the β -subunit interior and the orthosteric binding site, as Leu255 and Leu248 dominate the binding, being solely responsible for over 40% of the binding energy. This is followed by the mentioned Lys254 and Lys352 residues, which establish hydrogen bonds mainly with the cyano group and the unsaturated benzimidazole nitrogen atom, respectively, with the former occasionally being supported through Asn258 as well (Figure S128).

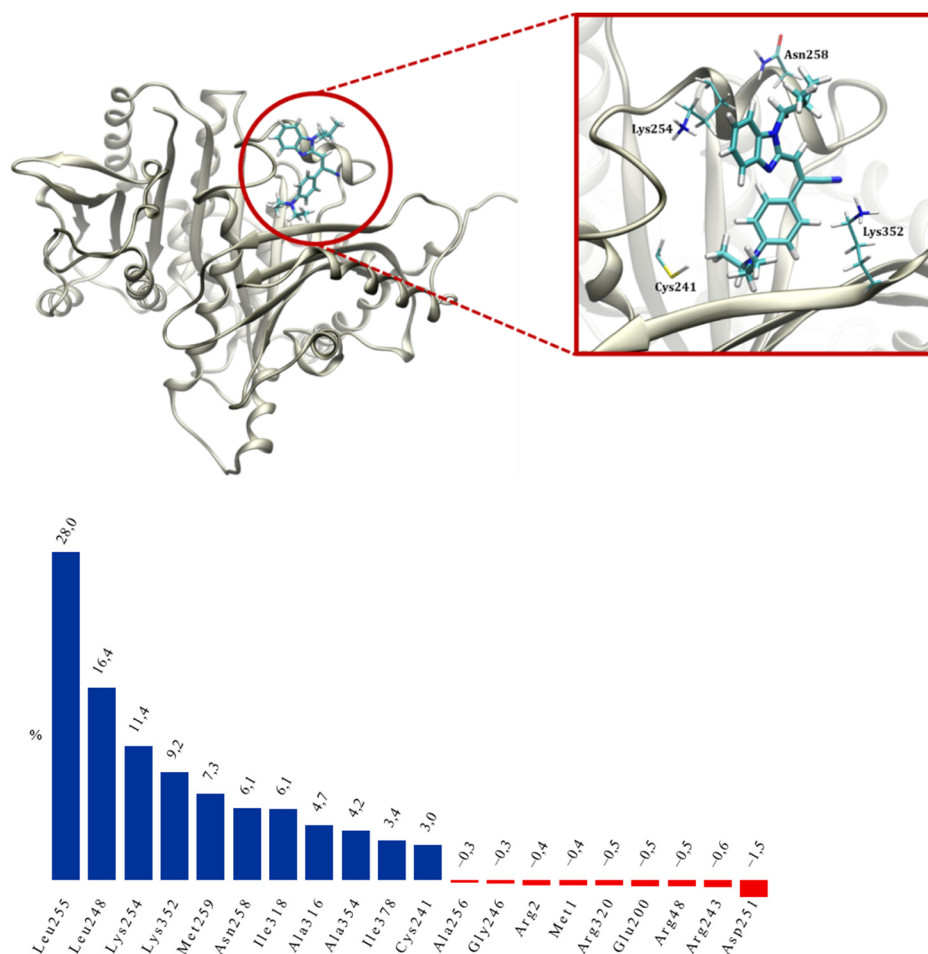


Figure 6. Representative structure of the *E*-isomer of **64** within the colchicine binding site (top) and relative contributions of individual residues to the overall binding free energy (bottom, in %), which lists all residues with favorable contributions higher than $-0.5 \text{ kcal mol}^{-1}$ (in blue) and unfavorable contributions exceeding $+0.1 \text{ kcal mol}^{-1}$ (in red).

In concluding this section, we can emphasize that docking simulations confirmed **64** as the most potent ligand studied here, while MD simulations support *E*-isomer as its biologically active form. The investigated ligands compete between orthosteric binding into the colchicine binding site responsible for the observed antitumor activities and other allosteric positions, where the latter prevails in several cases, leading to compounds that are inactive against tubulin polymerization; however, the obtained insights regarding the most potent systems suggest that higher tubulin affinities are associated with (i) bulkier alkyl and aryl moieties on the benzimidazole nitrogen and (ii) electron-donating substituents on the phenyl group that allow deeper entrance into the hydrophobic pocket within the β -subunit predominantly consisting of Leu255, Leu248, Met259, Ala354, and Ile378 residues.

3. Experimental Section

3.1. Chemistry

3.1.1. General Methods

All chemicals and solvents used for the synthesis were obtained from the commercial suppliers Aldrich and Acros. Melting points were determined on an SMP11 Bibby and Büchi 535 apparatus and were uncorrected. NMR spectra were taken in DMSO- d_6 solutions with TMS as an internal standard. The ^1H and ^{13}C NMR spectra were recorded on a Varian Bruker Advance III HD 400 MHz/54 mm Ascend instrument. Chemical shifts are given in ppm (δ) relative to TMS. All prepared compounds were checked by TLC with Merck silica gel 60F-254 glass plates. Microwave-assisted synthesis was performed in a Milestone start S microwave oven using quartz cuvettes under a pressure of 40 bar. Elemental analyses for C, H, and N were performed on a Perkin-Elmer 2400 elemental analyzer. Where analyses are indicated only as symbols of elements, the analytical results obtained were within 0.4% of the theoretical value. NMR spectra of newly prepared compounds are presented in Supporting Information (Figures S1–S119).

3.1.2. General Method for Preparation of Compounds 3–8

Compounds 3–8 were prepared using microwave irradiation at optimized reaction times at 170 °C, with a power level of 800 W and 40 bar pressure from 1 or 2 in acetonitrile (10 mL), with an excess of the corresponding amine. After cooling, the resulting product was purified by column chromatography on SiO_2 using dichloromethane/methanol at 200:1 as the eluent. The synthesis of the previously published derivatives 3–6 is outlined in the Supporting Materials.

N-Hexyl-2-nitroaniline 7

Compound 7 was prepared from 1 (0.50 g, 3.2 mmol) and hexylamine (2.90 mL, 22.2 mmol) after 2 h of irradiation to yield 0.69 g (98%) of orange oil. ^1H NMR (DMSO- d_6 , 400 MHz): δ /ppm = 8.12 (t, 1H, J = 5.1 Hz, NH), 8.06 (dd, 1H, J = 8.6, 1.6 Hz, H_{arom}), 7.54 (td, 1H, J = 7.8, 1.3 Hz, H_{arom}), 7.05 (d, 1H, J = 8.0 Hz, H_{arom}), 6.68 (td, 1H, J = 7.8, 1.3 Hz, H_{arom}), 3.37–3.34 (m, 2H, CH_2), 1.67–1.58 (m, 2H, CH_2), 1.41–1.26 (m, 6H, CH_2), 0.87 (t, 3H, J = 7.1 Hz, CH_3); ^{13}C NMR (DMSO- d_6 , 101 MHz): δ /ppm = 145.7, 137.1, 131.3, 126.7, 115.5, 115.0, 42.7, 31.4, 28.7, 26.5, 22.5, 14.3; Anal. Calcd. for $\text{C}_{12}\text{H}_{18}\text{N}_2\text{O}_2$: C, 64.84; H, 8.16; N, 12.60; O, 14.39. Found: C, 64.79; H, 8.12; N, 12.63; O, 14.32%.

3-*N*-(hexylamino)-4-nitrobenzotrile 8

Compound 8 was prepared from 2 (0.50 g, 2.7 mmol) and hexylamine (1.80 mL, 13.7 mmol) after 2 h of irradiation to yield 0.68 g (99%) of yellow oil. ^1H NMR (DMSO- d_6 , 300 MHz): δ /ppm = 8.58 (t, 1H, J = 5.4 Hz, NH), 8.50 (d, 1H, J = 2.0 Hz, H_{arom}), 7.81 (dd, 1H, J = 9.1, 1.6 Hz, H_{arom}), 7.18 (d, 1H, J = 9.1 Hz, H_{arom}), 3.41 (q, 2H, J = 6.7 Hz, CH_2), 1.65–1.55 (m, 2H, CH_2), 1.38–1.23 (m, 6H, CH_2), 0.87 (t, 3H, J = 6.7 Hz, CH_3); ^{13}C NMR (DMSO- d_6 , 75 MHz): δ /ppm = 146.8, 137.5, 131.9, 130.5, 118.2, 115.7, 96.0, 42.3, 30.8, 27.9, 25.8, 21.9, 13.7; Anal. Calcd. for $\text{C}_{13}\text{H}_{17}\text{N}_3\text{O}_2$: C, 63.14; H, 6.93; N, 16.99; O, 12.94. Found: C, 63.10; H, 6.97; N, 17.04; O, 12.88%.

3.1.3. General Method for Preparation of Compounds 9–11

Derivatives 3, 7, and 8 and a solution of $\text{SnCl}_2 \cdot 2\text{H}_2\text{O}$ in MeOH and concentrated HCl were refluxed for 0.5 h. After cooling, the reaction mixture was evaporated under vacuum conditions and dissolved in water (20 mL). The resulting solution was treated with 20% NaOH to pH = 14. The resulting precipitate was filtered off, washed with hot ethanol, then filtered again. The filtrate was evaporated at a reduced pressure and extracted with ethyl acetate. The organic layer was dried over anhydrous MgSO_4 and concentrated at reduced pressure. The synthesis of the previously published derivative 9 is outlined in Supporting Materials.

N-Hexylbenzene-1,2-diamine 10

Compound **10** was prepared from **7** (3.52 g, 15.8 mmol), SnCl₂·2H₂O (29.70 g, 131.6 mmol), HCl_{conc.} (49 mL), and MeOH (49 mL) to yield 2.14 g (70%) of brown oil. ¹H NMR (DMSO-d₆, 600 MHz): δ/ppm = 6.52 (dd, 1H, *J* = 7.8, 1.5 Hz, H_{arom}), 6.48 (td, 1H, *J* = 7.6, 1.5 Hz, H_{arom}), 6.41–6.37 (m, 2H, H_{arom}), 4.44 (s, 2H, NH₂), 4.28 (t, 1H, *J* = 5.2 Hz, NH), 2.99 (q, 2H, *J* = 6.9 Hz, CH₂), 1.61–1.55 (m, 2H, CH₂), 1.41–1.36 (m, 2H, CH₂), 1.31–1.28 (m, 4H, CH₂), 0.88 (t, 3H, *J* = 7.0 Hz, CH₃); ¹³C NMR (DMSO-d₆, 151 MHz): δ/ppm = 136.1, 135.0, 117.54, 116.5, 114.0, 109.6, 43.4, 31.2, 28.8, 26.5, 22.1, 13.2. Anal. Calcd. for C₁₂H₂₀N₂: C, 74.95; H, 10.48; N, 14.57. Found: C, 74.89; H, 10.54; N, 14.63%.

4-Amino-3-(hexylamino)benzonitrile **11**

Compound **11** was prepared from **8** (2.71 g, 10.9 mmol), SnCl₂·2H₂O (14.85 g, 131.6 mmol), HCl_{conc.} (29 mL), and MeOH (29 mL) to yield 1.65 g (69%) of yellow oil. ¹H NMR (DMSO-d₆, 300 MHz): δ/ppm = 6.91 (dd, 1H, *J* = 8.2, 1.9 Hz, H_{arom}), 6.76 (d, 1H, *J* = 2.0 Hz, H_{arom}), 6.44 (d, 1H, *J* = 8.2 Hz, H_{arom}), 5.32 (t, 1H, *J* = 5.0 Hz, NH), 4.96 (s, 2H, NH₂), 6.41–6.37 (m, 2H, H_{arom}), 4.44 (s, 2H, NH₂), 3.08 (q, 2H, *J* = 6.4 Hz, CH₂), 1.64–1.51 (m, 2H, CH₂), 1.39–1.27 (m, 6H, CH₂), 0.89 (t, 3H, *J* = 6.6 Hz, CH₃);

¹³C NMR (DMSO-d₆, 75 MHz): δ/ppm = 140.5, 135.5, 123.4, 121.6, 115.2, 108.8, 96.7, 43.2, 31.6, 28.8, 26.8, 22.6, 14.4. Anal. Calcd. for C₁₃H₁₉N₃: C, 71.85; H, 8.81; N, 19.34. Found: C, 71.81; H, 8.76; N, 19.37%.

3.1.4. General Method for Preparation of Compounds **14–16**

Benzonitrile derivatives **4–6** and a solution of SnCl₂·2H₂O in MeOH and concentrated HCl were refluxed for 0.5 h. After cooling, the reaction mixture was evaporated under vacuum conditions and dissolved in water (20 mL). The resulting solution was treated with 20% NaOH to pH = 14. The resulting precipitate was filtered off, washed with hot ethanol, then filtered again. The filtrate was evaporated at a reduced pressure, a small amount of water was added, then the product was filtered again. The synthesis of the previously published derivatives **14–16** is outlined in the Supporting Materials.

3.1.5. General Method for Preparation of Compounds **18–21**

A mixture of the corresponding substituted 1,2-phenylenediamines **9**, **10**, **12**, **13**, and 2-cyanoacetamide was heated in an oil bath for 35–50 min at 185 °C. After cooling, the resulting product was purified by column chromatography on SiO₂ using dichloromethane/methanol at 200:1 as the eluent. The synthesis of the previously published derivatives **18–20** is outlined in the Supporting Materials.

2-Cyanomethyl-*N*-hexylbenzimidazole **21**

Compound **21** was prepared from *N*-hexyl-1,2-phenylenediamine **10** (1.00 g, 5.2 mmol) and 2-cyanoacetamide (0.87 g, 10.4 mmol) after 40 min of heating to yield 0.24 g (20%) of brown oil. ¹H NMR (DMSO-d₆, 600 MHz): δ/ppm = 7.63 (d, 1H, *J* = 7.9 Hz, H_{arom}), 7.56 (d, 1H, *J* = 7.9 Hz, H_{arom}), 7.26 (td, 1H, *J* = 7.6, 1.0 Hz, H_{arom}), 7.21 (td, 1H, *J* = 7.6, 1.0 Hz, H_{arom}), 4.53 (s, 2H, NH₂), 4.20 (t, 2H, *J* = 7.5 Hz, CH₂), 1.75–1.67 (m, 2H, CH₂), 1.31–1.23 (m, 6H, CH₂), 0.84 (t, 3H, *J* = 7.0 Hz, CH₃); ¹³C NMR (DMSO-d₆, 75 MHz): δ/ppm = 145.6, 142.3, 135.7, 123.0, 122.3, 119.4, 116.9, 110.9, 43.7, 31.3, 29.6, 26.2, 22.4, 17.8, 14.3. Anal. Calcd. For C₁₅H₁₉N₃: C, 74.65; H, 7.94; N, 17.41. Found: C, 74.71; H, 7.90; N, 17.55%.

3.1.6. General Method for Preparation of Compounds **22–25**

A mixture of substituted benzonitriles **11**, **14–16**, and 2-cyanoacetamide was heated for 5–20 min at 280 °C. After cooling, the resulting product was purified by column chromatography on SiO₂ using dichloromethane/methanol at 200:1 as the eluent. The synthesis of the previously published derivatives **22–24** is outlined in the Supporting Materials.

6-Cyano-2-cyanomethyl-*N*-hexylbenzimidazole **25**

Compound **25** was prepared from 3-amino-4-*N*-hexylaminobenzonitrile **11** (0.50 g, 2.3 mmol) and 2-cyanoacetamide (0.39 g, 4.6 mmol) after 30 min of heating to yield 0.07 g (12%) of brown oil. ^1H NMR (DMSO- d_6 , 400 MHz): δ /ppm = 8.04 (d, 1H, J = 1.1 Hz, H_{arom}), 7.73 (d, 1H, J = 8.4 Hz, H_{arom}), 7.59 (dd, 1H, J = 8.4, 1.5 Hz, H_{arom}), 4.23 (t, 2H, J = 7.4 Hz, CH_2), 2.59 (s, 2H, CH_2), 1.74–1.66 (m, 2H, CH_2), 1.29–1.24 (m, 6H, CH_2), 0.83 (t, 3H, J = 7.0 Hz, CH_3); ^{13}C NMR (DMSO- d_6 , 101 MHz): δ /ppm = 155.4, 142.3, 138.7, 125.5, 123.4, 120.5 (2C), 111.9, 103.8, 43.8, 31.3, 29.6, 26.2, 22.4, 14.0. Anal. Calcd. for $\text{C}_{16}\text{H}_{18}\text{N}_4$: C, 72.15; H, 6.81; N, 21.04. Found: C, 72.23; H, 6.74; N, 20.93%.

3.1.7. General Method for Preparation of Compounds **32–71**

A solution of equimolar amounts of 2-(cyanomethyl)-benzimidazoles **17–25**, corresponding aromatic aldehydes **25–30**, and few drops of piperidine in absolute ethanol was refluxed for 2–4 h. The cooled reaction mixture was filtered, and if necessary the product was purified by column chromatography on SiO_2 using dichloromethane/methanol at 200:1 as the eluent.

(*E*)-2-(1*H*-benzimidazol-2-yl)-3-phenylacrylonitrile **32**

Compound **32** was prepared from **17** (0.10 g, 0.6 mmol) and **26** (0.07 g, 0.6 mmol) in absolute ethanol (2 mL) after refluxing for 2 h to yield 0.12 g (78%) of light yellow powder; m.p 224–228 °C; ^1H NMR (DMSO- d_6 , 400 MHz): δ /ppm = 13.10 (s, 1H, NH_{benz}), 8.36 (s, 1H, H_{arom}), 8.02–7.97 (m, 2H, H_{arom}), 7.71 (d, 1H, J = 7.9 Hz, H_{arom}), 7.64–7.55 (m, 4H, H_{arom}), 7.30 (t, 1H, J = 7.6 Hz, H_{arom}), 7.25 (t, 1H, J = 7.6 Hz, H_{arom}); ^{13}C NMR (DMSO- d_6 , 101 MHz): δ /ppm = 147.9, 145.8, 143.8, 135.3, 133.2, 132.2, 130.0 (2C), 129.9 (2C), 129.8, 124.2, 122.8, 119.7, 116.6, 112.0, 102.9; Anal. Calcd. for $\text{C}_{16}\text{H}_{11}\text{N}_3$: C, 78.35; H, 4.52; N, 17.13. Found: C, 78.43; H, 4.61; N, 17.07%.

(*E*)-2-(*N*-methylbenzimidazol-2-yl)-3-phenylacrylonitrile **33**

Compound **33** was prepared from **19** (0.10 g, 0.6 mmol) and **26** (0.06 g, 0.6 mmol) in absolute ethanol (2 mL) after refluxing for 2 h to yield 0.07 g (46%) of red oil. ^1H NMR (DMSO- d_6 , 400 MHz): δ /ppm = 8.19 (s, 1H, H_{arom}), 7.97–7.93 (m, 2H, H_{arom}), 7.80–7.76 (m, 1H, H_{arom}), 7.61–7.57 (m, 3H, H_{arom}), 7.34–7.31 (m, 3H, H_{arom}), 3.33 (s, 3H, CH_3); ^{13}C NMR (DMSO- d_6 , 101 MHz): δ /ppm = 166.8, 163.2, 151.0, 132.8, 132.4, 130.5, 130.2, 129.7, 129.5, 128.9, 128.3, 127.5, 119.3, 118.9, 116.9, 107.2, 30.3; Anal. Calcd. for $\text{C}_{17}\text{H}_{13}\text{N}_3$: C, 78.74; H, 5.05; N, 16.20. Found: C, 78.69; H, 4.95; N, 16.24%.

(*E*)-2-(*N*-phenylbenzimidazol-2-yl)-3-phenylacrylonitrile **34**

Compound **34** was prepared from **20** (0.10 g, 0.4 mmol) and **26** (0.05 g, 0.4 mmol) in absolute ethanol (2 mL) after refluxing for 2 h to yield 0.04 g (%) of red oil. ^1H NMR (DMSO- d_6 , 400 MHz): δ /ppm = 8.19 (s, 1H, H_{arom}), 7.96–7.93 (m, 3H, H_{arom}), 7.78 (bs, 1H, H_{arom}), 7.61–7.56 (m, 4H, H_{arom}), 7.50 (bs, 1H, H_{arom}), 7.42–7.26 (m, 5H, H_{arom}); ^{13}C NMR (DMSO- d_6 , 101 MHz): δ /ppm = 166.8, 163.2, 151.0 (2C), 137.4, 132.8 (2C), 132.4, 130.5 (2C), 129.7 (2C), 129.5, 129.2, 129.1, 129.1, 128.9, 128.8, 128.3, 127.5, 118.9, 117.0, 107.2; Anal. Calcd. for $\text{C}_{22}\text{H}_{15}\text{N}_3$: C, 82.22; H, 4.70; N, 13.08. Found: C, 82.15; H, 4.59; N, 13.24%.

(*E*)-2-(6-cyano-*N*-methylbenzimidazol-2-yl)-3-phenylacrylonitrile **35**

Compound **35** was prepared from **23** (0.10 g, 0.5 mmol) and **26** (0.05 g, 0.6 mmol) in absolute ethanol (2 mL) after refluxing for 2 h to yield 0.11 g (77%) of light brown powder; m.p 197–202 °C; ^1H NMR (DMSO- d_6 , 400 MHz): δ /ppm = 8.30 (d, 1H, J = 0.9 Hz, H_{arom}), 8.27 (s, 1H, H_{arom}), 8.09–8.04 (m, 2H, H_{arom}), 7.91 (d, 1H, J = 8.1 Hz, H_{arom}), 7.76 (dd, 1H, J = 8.5, 1.5 Hz, H_{arom}), 7.65–7.59 (m, 3H, H_{arom}), 4.07 (s, 3H, CH_3); ^{13}C NMR (DMSO- d_6 , 101 MHz): δ /ppm = 152.0, 150.6, 141.7, 139.9, 133.0, 132.7, 130.3 (2C), 129.7 (2C), 127.0, 124.8, 120.1, 116.9, 113.0, 105.4, 100.6, 32.6; Anal. Calcd. for $\text{C}_{18}\text{H}_{12}\text{N}_4$: C, 76.04; H, 4.25; N, 19.71. Found: C, 76.11; H, 4.14; N, 19.68%.

(*E*)-2-(6-cyano-*N*-phenylbenzimidazol-2-yl)-3-phenylacrylonitrile **36**

Compound **36** was prepared from **24** (0.10 g, 0.4 mmol) and **26** (0.04 g, 0.4 mmol) in absolute ethanol (2 mL) after refluxing for 2 h to yield 0.10 g (73%) of light yellow powder; m.p 195–200 °C; ¹H NMR (DMSO-d₆, 400 MHz): δ/ppm = 8.44 (s, 1H, H_{arom}), 7.98 (s, 1H, H_{arom}), 7.84–7.80 (m, 2H, H_{arom}), 7.73 (dd, 1H, J = 8.4, 1.3 Hz, H_{arom}), 7.71–7.66 (m, 5H, H_{arom}), 7.59–7.53 (m, 3H, H_{arom}), 7.39 (d, 1H, J = 8.5 Hz, H_{arom}); ¹³C NMR (DMSO-d₆, 101 MHz): δ/ppm = 152.3, 149.8, 141.9, 140.0, 134.8, 132.9, 132.6, 130.8 (2C), 130.5, 130.2 (2C), 129.7 (2C), 128.1 (2C), 128.0, 125.2, 119.9, 115.6, 112.8, 106.2, 100.3; Anal. Calcd. for C₂₃H₁₄N₄: C, 79.75; H, 4.07; N, 16.17. Found: C, 79.71; H, 4.14; N, 16.22%.

(E)-2-(1H-benzimidazol-2-yl)-3-(2-methoxyphenyl)acrylonitrile **37**

Compound **37** was prepared from **17** (0.10 g, 0.6 mmol) and **27** (0.09 g, 0.6 mmol) in absolute ethanol (3 mL) after refluxing for 3 h to yield 0.18 g (48%) of yellow powder; m.p 260–264 °C; ¹H NMR (DMSO-d₆, 600 MHz): δ/ppm = 13.11 (s, 1H, NH_{benz}), 8.54 (s, 1H, H_{arom}), 8.10 (dd, 1H, J = 7.8, 1.2 Hz, H_{arom}), 7.62 (bs, 1H, H_{arom}), 7.57 (td, 1H, J = 7.9, 1.6 Hz, H_{arom}), 7.28–7.24 (m, 2H, H_{arom}), 7.22 (d, 1H, J = 8.4 Hz, H_{arom}), 7.15 (t, 1H, J = 7.6 Hz, H_{arom}), 3.94 (s, 3H, OCH₃);

¹³C NMR (DMSO-d₆, 75 MHz): δ/ppm = 158.5, 148.0, 140.8, 133.9, 128.7, 121.9, 121.2, 116.7, 112.3, 103.3, 56.4; Anal. Calcd. for C₁₇H₁₃N₃O: C, 74.17; H, 4.76; N, 15.26; O, 5.81. Found: C, 74.11; H, 4.74; N, 15.31; O, 5.77%.

(E)-3-(2-methoxyphenyl)-2-(N-isobutylbenzimidazol-2-yl)acrylonitrile **38**

Compound **38** was prepared from **18** (0.10 g, 0.5 mmol) and **27** (0.06 g, 0.5 mmol) in absolute ethanol (3 mL) after refluxing for 4.5 h to yield 0.15 g (67%) of yellow oil in the form of a mixture of *E*- and *Z*-isomers at the ratio of 38a/38b = 2:1; 38a: ¹H NMR (DMSO-d₆, 400 MHz): δ/ppm = 8.42 (s, 1H, H_{arom}), 8.09 (dd, 1H, J = 7.8, 1.4 Hz, H_{arom}), 7.74–7.71 (m, 2H, H_{arom}), 7.62–7.58 (m, 1H, H_{arom}), 7.32–7.30 (m, 1H, H_{arom}), 7.28 (dd, 1H, J = 7.9, 1.3 Hz, H_{arom}), 7.23 (d, 1H, J = 7.9 Hz, H_{arom}), 7.18 (d, 1H, J = 7.7 Hz, H_{arom}), 4.35 (d, 2H, J = 7.5 Hz, CH₂), 3.92 (s, 3H, CH₃), 2.24–2.15 (m, 1H, CH), 0.87 (d, 6H, J = 6.7 Hz, CH₃); ¹³C NMR (DMSO-d₆, 101 MHz): δ/ppm = 158.6, 147.2, 146.4, 142.2, 136.9, 134.2, 128.6, 123.8, 123.1, 121.8, 121.2, 119.8, 117.1, 112.4, 111.2, 102.5, 56.5, 51.3, 29.8, 20.0; 38b: ¹H NMR (DMSO-d₆, 400 MHz): δ/ppm = 8.15 (s, 1H, H_{arom}), 7.76–7.73 (m, 1H, H_{arom}), 7.63 (dd, 1H, J = 6.9, 1.4 Hz, H_{arom}), 7.41 (td, 1H, J = 7.9, 1.7 Hz, H_{arom}), 7.36–7.32 (m, 2H, H_{arom}), 6.70 (t, 1H, J = 7.4 Hz, H_{arom}), 6.57 (dd, 1H, J = 7.8, 1.6 Hz, H_{arom}), 3.84 (s, 3H, CH₃), 3.64 (d, 2H, J = 7.6 Hz, CH₂), 2.06–2.00 (m, 1H, CH), 0.74 (d, 6H, J = 6.7 Hz, CH₃); ¹³C NMR (DMSO-d₆, 101 MHz): δ/ppm = 158.2, 146.8, 145.1, 142.8, 135.4, 134.0, 128.8, 124.0, 123.0, 121.8, 121.2, 121.0, 120.2, 118.6, 112.5, 112.1, 101.4, 56.5, 51.1, 29.0, 19.9; Anal. Calcd. for C₂₁H₂₁N₃O: C, 76.11; H, 6.39; N, 12.68; O, 4.83. Found: C, 76.28; H, 6.35; N, 12.71; O, 4.74%.

(E)-3-(2-methoxyphenyl)-2-(N-methylbenzimidazol-2-yl)acrylonitrile **39**

Compound **39** was prepared from **19** (0.10 g, 0.6 mmol) and **27** (0.08 g, 0.6 mmol) in absolute ethanol (3 mL) after refluxing for 3 h to yield 0.12 g (71%) of yellow powder; m.p 144–146 °C; ¹H NMR (DMSO-d₆, 400 MHz): δ/ppm = 8.33 (s, 1H, H_{arom}), 8.12 (dd, 1H, J = 7.8, 1.4 Hz, H_{arom}), 7.72 (d, 1H, J = 7.6 Hz, H_{arom}), 7.65 (d, 1H, J = 7.9 Hz, H_{arom}), 7.60 (td, 1H, J = 7.9, 1.4 Hz, H_{arom}), 7.36 (td, 1H, J = 7.6, 1.2 Hz, H_{arom}), 7.30 (td, 1H, J = 7.6, 1.1 Hz, H_{arom}), 7.22 (d, 1H, J = 8.4 Hz, H_{arom}), 7.17 (t, 1H, J = 7.6 Hz, H_{arom}), 4.01 (s, 3H, OCH₃), 3.92 (s, 3H, CH₃); ¹³C NMR (DMSO-d₆, 101 MHz): δ/ppm = 158.5, 147.8, 145.9, 142.3, 137.1, 134.1, 128.7, 123.8, 123.1, 121.9, 121.1, 119.7, 117.1, 112.3, 111.3, 101.4, 56.5, 32.1; Anal. Calcd. for C₁₈H₁₅N₃O: C, 74.72; H, 5.23; N, 14.52; O, 5.53. Found: C, 74.86; H, 5.04; N, 14.31; O, 5.77%.

(E)-3-(2-methoxyphenyl)-2-(N-phenylbenzimidazol-2-yl)acrylonitrile **40**

Compound **40** was prepared from **20** (0.10 g, 0.4 mmol) and **27** (0.06 g, 0.4 mmol) in absolute ethanol (3 mL) after refluxing for 2 h to yield 0.10 g (70%) of orange powder; m.p 169–173 °C; ¹H NMR (DMSO-d₆, 400 MHz): δ/ppm = 8.02 (dd, 1H, J = 7.8, 1.4 Hz, H_{arom}),

7.98 (s, 1H, H_{arom}), 7.84 (dd, 1H, *J* = 6.7, 1.5 Hz, H_{arom}), 7.72–7.65 (m, 3H, H_{arom}), 7.65–7.62 (m, 2H, H_{arom}), 7.53 (td, 1H, *J* = 7.8, 1.5 Hz, H_{arom}), 7.37 (td, 1H, *J* = 7.4, 1.5 Hz, H_{arom}), 7.33 (td, 1H, *J* = 7.5, 1.5 Hz, H_{arom}), 7.18 (dd, 1H, *J* = 6.9, 1.5 Hz, H_{arom}), 7.11 (d, 1H, *J* = 7.9 Hz, H_{arom}), 7.08 (d, 1H, *J* = 7.6 Hz, H_{arom}), 3.75 (s, 3H, CH₃); ¹³C NMR (DMSO-d₆, 101 MHz): δ/ppm = 158.5, 147.2, 144.5, 142.4, 137.6, 135.8, 134.3, 130.8 (2C), 129.9, 128.1, 128.0 (2C), 126.0, 124.8, 123.8, 121.4 (2C), 121.1, 120.1, 116.3 (2C), 112.3, 111.0, 101.3, 56.2; Anal. Calcd. for C₂₃H₁₇N₃O: C, 78.61; H, 4.88; N, 11.96; O, 4.55. Found: C, 78.51; H, 4.74; N, 11.81; O, 4.67%.

E-(*Z*)-2-(6-cyano-*N*-isobutylbenzimidazol-2-yl)-3-(2-methoxyphenyl)acrylonitrile **41**

Compound **41** was prepared from **22** (0.10 g, 0.4 mmol) and **27** (0.06 g, 0.4 mmol) in absolute ethanol (3 mL) after refluxing for 4.5 h to yield 0.15 g (30%) of yellow oil in the form of a mixture of *E*- and *Z*-isomers at a ratio of 41a/41b = 2:1; 41a: ¹H NMR (DMSO-d₆, 600 MHz): δ/ppm = 8.33 (d, 1H, *J* = 1.08 Hz, H_{arom}), 8.21 (s, 1H, H_{arom}), 7.88 (d, 1H, *J* = 8.45 Hz, H_{arom}), 7.75–7.73 (m, 1H, H_{arom}), 7.42 (td, 1H, *J* = 7.9, 1.6 Hz, H_{arom}), 7.13 (d, 1H, *J* = 8.3 Hz, H_{arom}), 6.73 (t, 1H, *J* = 7.5 Hz, H_{arom}), 6.60 (dd, 1H, *J* = 7.8, 1.3 Hz, H_{arom}), 3.77 (s, 3H, CH₃), 3.69 (d, 2H, *J* = 7.6 Hz, CH₂), 2.05–1.96 (m, 1H, CH), 0.73 (d, 6H, *J* = 6.6 Hz, CH₃);

¹³C NMR (DMSO-d₆, 151 MHz): δ/ppm = 158.2, 149.4, 147.2, 141.1, 139.3, 134.1, 128.2, 126.4, 124.5, 121.1, 120.7, 119.6, 116.3, 113.1, 112.0, 105.0, 100.0, 56.0, 51.1, 29.3, 19.4 (2C); 41b: ¹H NMR (DMSO-d₆, 600 MHz): δ/ppm = 8.51 (s, 1H, H_{arom}), 8.30 (d, 1H, *J* = 1.0 Hz, H_{arom}), 8.10 (dd, 1H, *J*₁ = 7.7, 1.3 Hz, H_{arom}), 7.96 (d, 1H, *J* = 8.6 Hz, H_{arom}), 7.73–7.71 (m, 1H, H_{arom}), 7.61 (td, 1H, *J* = 7.7, 1.6 Hz, H_{arom}), 7.23 (d, 1H, *J* = 8.4 Hz, H_{arom}), 7.17 (t, 1H, *J* = 7.5 Hz, H_{arom}), 4.40 (d, 2H, *J* = 7.5 Hz, CH₂), 3.92 (s, 3H, CH₃), 2.22–2.16 (m, 1H, CH), 0.86 (d, 6H, *J* = 6.6 Hz, CH₃); ¹³C NMR (DMSO-d₆, 151 MHz): δ/ppm = 158.8, 148.8, 147.7, 141.7, 137.8, 133.8, 128.6, 126.7, 124.9, 121.1, 120.5, 119.4, 117.7, 113.2, 112.0, 105.0, 101.2, 56.0, 50.6, 28.6, 19.4 (2C); Anal. Calcd. for C₂₂H₂₀N₄O: C, 74.14; H, 5.66; N, 15.72; O, 4.49. Found: C, 74.11; H, 5.74; N, 15.75; O, 4.54%.

E)-2-(6-cyano-*N*-methylbenzimidazol-2-yl)-3-(2-methoxyphenyl)acrylonitrile **42**

Compound **42** was prepared from **23** (0.10 g, 0.5 mmol) and **27** (0.10 g, 0.5 mmol) in absolute ethanol (3 mL) after refluxing for 3 h to yield 0.13 g (80%) of brown powder; m.p 178–181 °C; ¹H NMR (DMSO-d₆, 400 MHz): δ/ppm = 8.41 (s, 1H, H_{arom}), 8.30 (d, 1H, *J* = 1.0 Hz, H_{arom}), 8.13 (dd, 1H, *J* = 7.4, 1.4 Hz, H_{arom}), 7.88 (d, 1H, *J* = 8.4 Hz, H_{arom}), 7.75 (dd, 1H, *J* = 8.5, 1.4 Hz, H_{arom}), 7.62 (td, 1H, *J* = 7.9, 1.4 Hz, H_{arom}), 7.23 (d, 1H, *J* = 8.1 Hz, H_{arom}), 7.18 (t, 1H, *J* = 7.6 Hz, H_{arom}), 4.05 (s, 3H, OCH₃), 3.92 (s, 3H, CH₃); ¹³C NMR (DMSO-d₆, 101 MHz): δ/ppm = 158.7, 150.6, 147.1, 141.7, 139.9, 134.5, 128.7, 126.9, 124.8, 121.7, 121.2, 120.2, 116.8, 113.0, 112.4, 105.3, 100.7, 56.5, 32.6; Anal. Calcd. for C₁₉H₁₄N₄O: C, 72.60; H, 4.49; N, 17.82; O, 5.09. Found: C, 72.53; H, 4.41; N, 17.75; O, 4.94%.

E)-2-(6-cyano-*N*-phenylbenzimidazol-2-yl)-3-(2-methoxyphenyl)acrylonitrile **43**

Compound **43** was prepared from **24** (0.10 g, 0.4 mmol) and **27** (0.05 g, 0.4 mmol) in absolute ethanol (3 mL) after refluxing for 2 h to yield 0.15 g (77%) of yellow powder; m.p 222–225 °C; ¹H NMR (DMSO-d₆, 400 MHz): δ/ppm = 8.44 (d, 1H, *J* = 0.9 Hz, H_{arom}), 8.06–8.01 (m, 2H, H_{arom}), 7.73–7.67 (m, 6H, H_{arom}), 7.55 (td, 1H, *J* = 7.9, 1.4 Hz, H_{arom}), 7.32 (dd, 1H, *J* = 8.4, 0.5 Hz, H_{arom}), 7.12 (d, 1H, *J* = 8.6 Hz, H_{arom}), 7.08 (d, 1H, *J* = 7.5 Hz, H_{arom}), 3.75 (s, 3H, CH₃); ¹³C NMR (DMSO-d₆, 101 MHz): δ/ppm = 158.6, 149.9, 145.8, 141.9, 140.3, 135.1, 134.7, 130.9 (2C), 130.5, 128.2, 128.1 (2C), 127.9, 126.1, 125.1, 121.1, 119.9, 116.0, 112.6, 112.4, 106.0 (2C), 100.5, 56.2; Anal. Calcd. for C₂₄H₁₆N₄O: C, 76.58; H, 4.28; N, 14.88; O, 4.25. Found: C, 76.61; H, 4.24; N, 15.05; O, 4.34%.

E)-2-(1*H*-benzimidazol-2-yl)-3-(2,4-dimethoxyphenyl)acrylonitrile **44**

Compound **44** was prepared from **17** (0.10 g, 0.6 mmol) and **28** (0.10 g, 0.6 mmol) in absolute ethanol (3 mL) after refluxing for 3 h to yield 0.19 g (80%) of yellow powder; m.p 205–209 °C; ¹H NMR (DMSO-d₆, 600 MHz): δ/ppm = 13.00 (s, 1H, NH_{benz}), 8.47 (s, 1H,

H_{arom}), 8.17 (d, 1H, $J = 8.7$ Hz, H_{arom}), 7.62 (bs, 2H, H_{arom}), 7.23 (bs, 2H, H_{arom}), 6.76 (dd, 1H, $J = 8.8, 2.3$ Hz, H_{arom}), 6.74 (d, 1H, $J = 2.3$ Hz, H_{arom}), 3.95 (s, 3H, OCH₃), 3.88 (s, 3H, OCH₃); ¹³C NMR (DMSO-d₆, 151 MHz): δ /ppm = 164.0, 160.0, 148.0, 139.5, 129.2, 116.9, 114.3, 106.4, 98.9, 98.4, 56.1, 55.7; Anal. Calcd. for C₁₈H₁₅N₃O₂: C, 70.81; H, 4.95; N, 13.76; O, 10.48. Found: C, 70.78; H, 4.74; N, 13.75; O, 10.54%.

E-(*Z*)-3-(2,4-dimethoxyphenyl)-2-(*N*-isobutylbenzimidazol-2-yl)acrylonitrile 45

Compound 45 was prepared from 18 (0.10 g, 0.5 mmol) and 28 (0.08 g, 0.5 mmol) in absolute ethanol (3 mL) after refluxing for 4 h to yield 0.12 g (70%) of yellow oil in the form of a mixture of *E*- and *Z*-isomers at a ratio of 45a/45b = 5:1; 45a: ¹H NMR (DMSO-d₆, 600 MHz): δ /ppm = 8.33 (s, 1H, H_{arom}), 8.16 (d, 1H, $J = 8.8$ Hz, H_{arom}), 7.67–7.63 (m, 2H, H_{arom}), 7.28–7.26 (m, 1H, H_{arom}), 7.25–7.21 (m, 1H, H_{arom}), 6.75 (dd, 1H, $J = 8.8, 2.3$ Hz, H_{arom}), 6.71 (d, 1H, $J = 2.3$ Hz, H_{arom}), 4.29 (d, 2H, $J = 7.4$ Hz, CH₂), 3.88 (s, 3H, OCH₃), 3.86 (s, 3H, OCH₃), 2.19–2.11 (m, 1H, CH), 0.82 (d, 6H, $J = 6.6$ Hz, CH₃); ¹³C NMR (DMSO-d₆, 151 MHz): δ /ppm = 164.3, 160.2, 147.4, 144.7, 141.7, 136.4, 129.2, 123.0, 122.5, 119.1, 117.4, 114.1, 111.3, 106.5, 98.4, 96.6, 56.1, 55.8, 50.8, 29.2, 19.5 (2C); 45b: ¹H NMR (DMSO-d₆, 600 MHz): δ /ppm = 7.98 (s, 1H, H_{arom}), 7.70 (d, 1H, $J = 7.8$ Hz, H_{arom}), 7.61 (d, 1H, $J = 8.0$ Hz, H_{arom}), 7.31–7.28 (m, 2H, H_{arom}), 6.61 (d, 1H, $J = 2.3$ Hz, H_{arom}), 6.43 (d, 1H, $J = 8.8$ Hz, H_{arom}), 6.29 (dd, 1H, $J = 8.8, 2.3$ Hz, H_{arom}), 6.71 (d, 1H, $J = 2.3$ Hz, H_{arom}), 3.81 (s, 3H, OCH₃), 3.71 (s, 3H, OCH₃), 3.68 (d, 2H, $J = 7.4$ Hz, CH₂), 2.05–1.98 (m, 1H, CH), 0.72 (d, 6H, $J = 6.6$ Hz, CH₃); ¹³C NMR (DMSO-d₆, 151 MHz): δ /ppm = 164.0, 159.8, 145.1, 144.9, 142.4, 134.9, 129.5, 129.2, 123.0, 119.7, 118.7, 114.0, 111.5, 106.5, 98.4, 56.2, 55.6, 50.7, 28.6, 19.5 (2C); Anal. Calcd. for C₂₂H₂₃N₃O₂: C, 73.11; H, 6.41; N, 11.63; O, 8.85. Found: C, 73.19; H, 6.51; N, 11.58; O, 8.75%.

(*E*)-3-(2,4-dimethoxyphenyl)-2-(*N*-methylbenzimidazol-2-yl)acrylonitrile 46

Compound 46 was prepared from 19 (0.10 g, 0.6 mmol) and 28 (0.09 g, 0.6 mmol) in absolute ethanol (3 mL) after refluxing for 3 h to yield 0.19 g (89%) of yellow powder; m.p 168–171 °C; ¹H NMR (DMSO-d₆, 600 MHz): δ /ppm = 8.26 (s, 1H, H_{arom}), 8.20 (d, 1H, $J = 8.7$ Hz, H_{arom}), 7.68 (d, 1H, $J = 8.0$ Hz, H_{arom}), 7.61 (d, 1H, $J = 8.0$ Hz, H_{arom}), 7.32 (td, 1H, $J = 7.7, 1.0$ Hz, H_{arom}), 7.27 (td, 1H, $J = 7.8, 1.0$ Hz, H_{arom}), 6.78 (dd, 1H, $J = 8.8, 2.4$ Hz, H_{arom}), 6.73 (d, 1H, $J = 2.3$ Hz, H_{arom}), 3.97 (s, 3H, OCH₃), 3.91 (s, 3H, OCH₃), 3.89 (s, 3H, CH₃); ¹³C NMR (DMSO-d₆, 151 MHz): δ /ppm = 164.2, 160.1, 148.0, 144.4, 141.9, 136.6, 129.2, 123.0, 122.5, 119.0, 117.3, 114.2, 110.6, 106.5, 98.4, 96.7, 56.1, 55.7, 31.5; Anal. Calcd. for C₁₉H₁₇N₃O₂: C, 71.46; H, 5.37; N, 13.16; O, 10.02. Found: C, 71.39; H, 5.43; N, 13.07; O, 10.13%.

(*E*)-3-(2,4-dimethoxyphenyl)-2-(*N*-phenylbenzimidazol-2-yl)acrylonitrile 47

Compound 47 was prepared from 20 (0.10 g, 0.4 mmol) and 28 (0.07 g, 0.4 mmol) in absolute ethanol (3 mL) after refluxing for 4 h to yield 0.16 g (75%) of yellow powder; m.p 164–166 °C; ¹H NMR (DMSO-d₆, 600 MHz): δ /ppm = 8.10 (d, 1H, $J = 8.8$ Hz, H_{arom}), 7.95 (s, 1H, H_{arom}), 7.80 (d, 1H, $J = 7.9$ Hz, H_{arom}), 7.69–7.62 (m, 3H, H_{arom}), 7.59 (dd, 2H, $J = 6.9, 1.5$ Hz, H_{arom}), 7.34 (td, 1H, $J = 8.1, 1.1$ Hz, H_{arom}), 7.30 (td, 1H, $J = 7.9, 1.0$ Hz, H_{arom}), 7.14 (d, 1H, $J = 7.9$ Hz, H_{arom}), 6.70 (dd, 1H, $J = 8.9, 2.3$ Hz, H_{arom}), 6.63 (d, 1H, $J = 2.3$ Hz, H_{arom}), 3.85 (s, 3H, OCH₃), 3.75 (s, 3H, OCH₃); ¹³C NMR (DMSO-d₆, 75 MHz): δ /ppm = 164.7, 160.5, 147.9, 143.5, 142.4, 137.6, 136.0, 130.7, 129.9, 129.2, 128.0, 124.5, 123.7, 119.9, 117.0, 114.3, 110.9, 107.0, 98.7, 97.2, 56.4, 56.2, 56.1; Anal. Calcd. for C₂₄H₁₉N₃O₂: C, 75.57; H, 5.02; N, 11.02; O, 8.39. Found: C, 75.51; H, 4.92; N, 11.08; O, 8.22%.

(*E*)-2-(6-cyano-*N*-isobutylbenzimidazol-2-yl)-3-(2,4-dimethoxyphenyl)acrylonitrile 48

Compound 48 was prepared from 22 (0.10 g, 0.4 mmol) and 28 (0.07 g, 0.4 mmol) in absolute ethanol (3 mL) after refluxing for 4 h to yield 0.16 g (84%) of orange powder; m.p 120–125 °C; ¹H NMR (DMSO-d₆, 600 MHz): δ /ppm = 8.43 (s, 1H, H_{arom}), 8.23 (d, 1H, $J = 0.9$ Hz, H_{arom}), 8.18 (d, 1H, $J = 8.8$ Hz, H_{arom}), 7.89 (d, 1H, $J = 8.5$ Hz, H_{arom}), 7.67 (dd, 1H, $J = 8.5, 1.4$ Hz, H_{arom}), 6.75 (dd, 1H, $J = 8.8, 2.3$ Hz, H_{arom}), 6.71 (d, 1H, $J = 2.3$ Hz,

H_{arom}), 4.35 (d, 2H, $J = 7.6$ Hz, CH_2), 3.89 (s, 3H, OCH_3), 3.86 (s, 3H, OCH_3), 2.18–2.10 (m, 1H, CH), 0.82 (d, 6H, $J = 6.6$ Hz, CH_3); ^{13}C NMR (DMSO- d_6 , 151 MHz): $\delta/\text{ppm} = 164.2, 159.8, 148.2, 146.2, 141.8, 137.8, 129.9, 126.6, 124.8, 119.5, 118.4, 113.8, 113.2, 106.7, 104.9, 98.4, 97.2, 56.2, 55.7, 50.9, 28.7, 19.4$ (2C); Anal. Calcd. for $\text{C}_{23}\text{H}_{22}\text{N}_4\text{O}_2$: C, 71.48; H, 5.74; N, 14.50; O, 8.28. Found: C, 71.54; H, 5.61; N, 14.58; O, 8.15%.

(*E*)-2-(6-cyano-*N*-methylbenzimidazol-2-yl)-3-(2,4-dimethoxyphenyl)acrylonitrile **49**

Compound **49** was prepared from **23** (0.10 g, 0.5 mmol) and **28** (0.08 g, 0.5 mmol) in absolute ethanol (3 mL) after refluxing for 2 h to yield 0.17 g (77%) of yellow powder; m.p 228–231 °C; ^1H NMR (DMSO- d_6 , 400 MHz): $\delta/\text{ppm} = 8.37$ (s, 1H, H_{arom}), 8.26 (d, 1H, $J = 0.9$ Hz, H_{arom}), 8.23 (d, 1H, $J = 8.8$ Hz, H_{arom}), 7.85 (d, 1H, $J = 8.4$ Hz, H_{arom}), 7.72 (dd, 1H, $J = 8.5, 1.4$ Hz, H_{arom}), 6.80 (dd, 1H, $J = 8.8, 2.3$ Hz, H_{arom}), 6.75 (d, 1H, $J = 2.4$ Hz, H_{arom}), 4.03 (s, 3H, OCH_3), 3.93 (s, 3H, OCH_3), 3.91 (s, 3H, CH_3); ^{13}C NMR (DMSO- d_6 , 151 MHz): $\delta/\text{ppm} = 165.1, 160.9, 151.3, 146.0, 141.8, 140.0, 129.9, 126.6, 124.5, 120.2, 117.6, 114.5, 112.8, 107.1, 105.1, 98.9, 96.2, 56.7, 56.3, 32.5$; Anal. Calcd. for $\text{C}_{20}\text{H}_{16}\text{N}_4\text{O}_2$: C, 69.76; H, 4.68; N, 16.27; O, 9.29. Found: C, 69.71; H, 4.51; N, 16.38; O, 9.15%.

(*E*)-2-(6-cyano-*N*-phenylbenzimidazol-2-yl)-3-(2,4-dimethoxyphenyl)acrylonitrile **50**

Compound **50** was prepared from **24** (0.10 g, 0.4 mmol) and **28** (0.06 g, 0.4 mmol) in absolute ethanol (3 mL) after refluxing for 2 h to yield 0.16 g (98%) of yellow powder; m.p 213–217 °C; ^1H NMR (DMSO- d_6 , 400 MHz): $\delta/\text{ppm} = 8.39$ (d, 1H, $J = 0.8$ Hz, H_{arom}), 8.13 (d, 1H, $J = 8.9$ Hz, H_{arom}), 8.02 (s, 1H, H_{arom}), 7.70–7.65 (m, 6H, H_{arom}), 7.28 (d, 1H, $J = 8.5$ Hz, H_{arom}), 6.71 (dd, 1H, $J = 8.9, 2.3$ Hz, H_{arom}), 6.64 (d, 1H, $J = 2.4$ Hz, H_{arom}), 3.86 (s, 3H, OCH_3), 3.76 (s, 3H, OCH_3); ^{13}C NMR (DMSO- d_6 , 151 MHz): $\delta/\text{ppm} = 164.4, 153.4, 150.9, 133.1$ (2C), 119.2, 118.7, 112.1 (2C), 97.7, 40.0 (2C); Anal. Calcd. for $\text{C}_{25}\text{H}_{18}\text{N}_4\text{O}_2$: C, 73.88; H, 4.46; N, 13.78; O, 7.87. Found: C, 73.73; H, 4.51; N, 13.69; O, 7.75%.

(*E*)-2-(1*H*-benzimidazol-2-yl)-3-(3,4,5-trimethoxyphenyl)acrylonitrile **51**

Compound **51** was prepared from **17** (0.10 g, 0.6 mmol) and **29** (0.12 g, 0.6 mmol) in absolute ethanol (3 mL) after refluxing for 2.5 h to yield 0.05 g (22%) of yellow powder; m.p 188–193 °C; ^1H NMR (DMSO- d_6 , 400 MHz): $\delta/\text{ppm} = 8.17$ (s, 1H, H_{arom}), 7.85 (bs, 1H, H_{arom}), 7.74 (bs, 2H, H_{arom}), 7.36 (s, 3H, H_{arom}), 3.83 (s, 6H, OCH_3), 3.77 (s, 3H, OCH_3); ^{13}C NMR (DMSO- d_6 , 101 MHz): $\delta/\text{ppm} = 163.2, 153.4, 151.3, 141.5, 127.6, 117.3, 108.4, 105.5, 60.8, 56.5$; Anal. Calcd. for $\text{C}_{19}\text{H}_{17}\text{N}_3\text{O}_3$: C, 68.05; H, 5.11; N, 12.53; O, 14.31. Found: C, 68.11; H, 4.96; N, 12.38; O, 14.36%.

(*E*)-2-(*N*-isobutylbenzimidazol-2-yl)-3-(3,4,5-trimethoxyphenyl)acrylonitrile **52**

Compound **52** was prepared from **18** (0.10 g, 0.5 mmol) and **29** (0.09 g, 0.5 mmol) in absolute ethanol (3 mL) after refluxing for 4 h to yield 0.18 g (64%) of orange oil; ^1H NMR (DMSO- d_6 , 400 MHz): $\delta/\text{ppm} = 8.25$ (s, 1H, H_{arom}), 7.72 (t, 2H, $J = 8.3$ Hz, H_{arom}), 7.50 (s, 1H, H_{arom}), 7.35–7.28 (m, 2H, H_{arom}), 4.36 (d, 2H, $J = 7.4$ Hz, CH_2), 3.87 (s, 6H, OCH_3), 3.79 (s, 3H, OCH_3), 2.21–2.13 (m, 1H, CH), 0.84 (d, 6H, $J = 6.7$ Hz, CH_3); ^{13}C NMR (DMSO- d_6 , 101 MHz): $\delta/\text{ppm} = 153.4, 153.0, 151.5, 147.3, 142.2, 136.9, 128.4, 128.1, 123.8, 123.1, 119.7, 117.6, 112.0, 108.2, 107.8, 99.1, 60.8, 56.5$ (2C), 55.7, 51.3, 20.0 (2C); Anal. Calcd. for $\text{C}_{23}\text{H}_{25}\text{N}_3\text{O}_3$: C, 70.57; H, 6.44; N, 10.73; O, 12.26. Found: C, 70.62; H, 6.41; N, 10.81; O, 12.36%.

(*E*)-3-(3,4,5-trimethoxyphenyl)-2-(*N*-methylbenzimidazol-2-yl)acrylonitrile **53**

Compound **53** was prepared from **19** (0.10 g, 0.6 mmol) and **29** (0.11 g, 0.6 mmol) in absolute ethanol (3 mL) after refluxing for 4 h to yield 0.20 g (49%) of yellow powder; m.p 134–137 °C; ^1H NMR (DMSO- d_6 , 400 MHz): $\delta/\text{ppm} = 8.13$ (s, 1H, H_{arom}), 7.71 (d, 1H, $J = 7.7$ Hz, H_{arom}), 7.67 (d, 1H, $J = 7.9$ Hz, H_{arom}), 7.49 (s, 2H, H_{arom}), 7.36 (td, 1H, $J = 7.6, 1.1$ Hz, H_{arom}), 7.30 (td, 1H, $J = 7.5, 1.1$ Hz, H_{arom}), 4.02 (s, 3H, OCH_3), 3.87 (s, 3H, OCH_3), 3.79 (s, 3H, OCH_3); ^{13}C NMR (DMSO- d_6 , 101 MHz): $\delta/\text{ppm} = 153.4, 150.6, 147.9, 142.4, 141.2, 137.1, 128.5, 123.8, 123.1, 119.7, 117.6, 111.3, 108.1, 99.7, 60.8, 56.5$ (2C), 32.2; Anal.

Calcd. for C₂₀H₁₉N₃O₃: C, 68.75; H, 5.48; N, 12.03; O, 13.74. Found: C, 68.72; H, 5.36; N, 12.08; O, 13.66%.

(*E*)-2-(*N*-phenylbenzimidazol-2-yl)-3-(3,4,5-trimethoxyphenyl)acrylonitrile **54**

Compound **54** was prepared from **20** (0.10 g, 0.4 mmol) and **29** (0.08 g, 0.4 mmol) in absolute ethanol (3 mL) after refluxing for 4 h to yield 0.17 g (71%) of orange oil; ¹H NMR (DMSO-d₆, 300 MHz): δ/ppm = 7.99 (s, 1H, H_{arom}), 7.81 (d, 1H, *J* = 6.8 Hz, H_{arom}), 7.67–7.62 (m, 3H, H_{arom}), 7.51–7.46 (m, 1H, H_{arom}), 7.38–7.33 (m, 2H, H_{arom}), 7.27 (s, 2H, H_{arom}), 7.22 (d, 1H, *J* = 7.2 Hz, H_{arom}), 7.13–7.10 (m, 1H, H_{arom}), 3.79 (s, 3H, OCH₃), 3.75 (s, 3H, OCH₃); ¹³C NMR (DMSO-d₆, 101 MHz): δ/ppm = 153.3, 153.0, 152.5, 151.0, 135.5, 134.6, 130.7, 130.6, 130.2, 130.2, 129.2, 128.0, 126.4, 126.3, 125.2, 124.0, 123.9, 120.4, 107.6, 107.5, 60.8, 60.7, 56.5, 55.8, 55.7; Anal. Calcd. for C₂₅H₂₁N₃O₃: C, 72.98; H, 5.14; N, 10.21; O, 11.67. Found: C, 72.86; H, 5.06; N, 10.18; O, 11.59%.

(*E*)-2-(6-cyano-*N*-isobutylbenzimidazol-2-yl)-3-(3,4,5-trimethoxyphenyl)acrylonitrile **55**

Compound **55** was prepared from **22** (0.10 g, 0.4 mmol) and **29** (0.08 g, 0.4 mmol) in absolute ethanol (3 mL) after refluxing for 4 h to yield 0.17 g (56%) of yellow powder; m.p 163–167 °C; ¹H NMR (DMSO-d₆, 600 MHz): δ/ppm = 8.33 (s, 1H, H_{arom}), 8.28 (d, 1H, *J* = 1.2 Hz, H_{arom}), 7.98 (d, 1H, *J* = 8.4 Hz, H_{arom}), 7.74 (dd, 1H, *J* = 8.5, 1.4 Hz, H_{arom}), 7.51 (s, 2H, H_{arom}), 4.43 (d, 2H, *J* = 7.6 Hz, CH₂), 3.86 (s, 6H, OCH₃), 3.80 (s, 3H, OCH₃), 2.20–2.15 (m, 1H, CH), 0.84 (d, 6H, *J* = 6.6 Hz, CH₃); ¹³C NMR (DMSO-d₆, 151 MHz): δ/ppm = 152.9, 152.3, 149.5, 141.2, 141.1, 139.3, 127.6, 126.4, 124.3, 119.5, 116.7, 113.1, 108.0, 105.0, 97.7, 60.3, 56.0 (2C), 51.0, 29.3, 19.4; Anal. Calcd. for C₂₄H₂₄N₄O₃: C, 69.21; H, 5.81; N, 13.45; O, 11.52. Found: C, 69.19; H, 5.86; N, 13.38; O, 11.56%.

(*E*)-2-(6-cyano-*N*-methylbenzimidazol-2-yl)-3-(3,4,5-trimethoxyphenyl)acrylonitrile **56**

Compound **56** was prepared from **23** (0.10 g, 0.5 mmol) and **29** (0.09 g, 0.5 mmol) in absolute ethanol (3 mL) after refluxing for 4 h to yield 0.16 g (88%) of yellow powder; m.p 259–262 °C; ¹H NMR (DMSO-d₆, 400 MHz): δ/ppm = 8.28 (d, 1H, *J* = 1.0 Hz, H_{arom}), 8.19 (s, 1H, H_{arom}), 7.89 (d, 1H, *J* = 8.5 Hz, H_{arom}), 7.75 (dd, 1H, *J* = 8.5, 1.5 Hz, H_{arom}), 7.50 (s, 2H, H_{arom}), 4.06 (s, 3H, OCH₃), 3.87 (s, 3H, OCH₃), 3.80 (s, 3H, OCH₃); ¹³C NMR (DMSO-d₆, 101 MHz): δ/ppm = 153.4, 151.8, 150.7, 141.7, 141.5, 139.9, 128.2, 126.9, 124.7, 120.2, 117.3, 113.0, 108.3, 105.3, 98.9, 60.8, 56.5 (2C), 32.6; Anal. Calcd. for C₂₁H₁₈N₄O₃: C, 67.37; H, 4.85; N, 14.96; O, 12.82. Found: C, 67.29; H, 4.89; N, 14.88; O, 12.86%.

(*E*)-2-(6-cyano-*N*-phenylbenzimidazol-2-yl)-3-(3,4,5-trimethoxyphenyl)acrylonitrile **57**

Compound **57** was prepared from **24** (0.10 g, 0.4 mmol) and **29** (0.08 g, 0.4 mmol) in absolute ethanol (3 mL) after refluxing for 4 h to yield 0.17 g (83%) of yellow powder; m.p 147–150 °C; ¹H NMR (DMSO-d₆, 600 MHz): δ/ppm = 8.39 (d, 1H, *J* = 0.9 Hz, H_{arom}), 8.06 (s, 1H, H_{arom}), 7.71 (dd, 1H, *J* = 8.5, 1.4 Hz, H_{arom}), 7.69–7.66 (m, 5H, H_{arom}), 7.36 (d, 1H, *J* = 8.4 Hz, H_{arom}), 7.29 (s, 2H, H_{arom}), 3.79 (s, 3H, OCH₃), 3.76 (s, 3H, OCH₃); ¹³C NMR (DMSO-d₆, 75 MHz): δ/ppm = 153.4, 152.3, 145.0, 141.9, 140.1, 134.8, 130.7, 130.5, 128.1, 127.9, 127.9, 124.9, 119.9, 115.9, 112.7, 108.2, 106.1, 98.4, 60.8, 56.5 (2C); Anal. Calcd. for C₂₆H₂₀N₄O₃: C, 71.55; H, 4.62; N, 12.84; O, 11.00. Found: C, 71.48; H, 4.65; N, 12.78; O, 11.07%.

(*E*)-2-(1*H*-benzimidazol-2-yl)-3-(4-*N,N*-dimethylaminophenyl)acrylonitrile **58**

Compound **58** was prepared from **17** (0.10 g, 0.6 mmol) and **30** (0.09 g, 0.6 mmol) in absolute ethanol (2 mL) after refluxing for 3 h to yield 0.14 g (76%) of orange powder; m.p 272–277 °C; ¹H NMR (DMSO-d₆, 300 MHz): δ/ppm = 12.78 (s, 1H, NH_{benz}), 8.13 (s, 1H, H_{arom}), 7.91 (d, 1H, *J* = 9.0 Hz, H_{arom}), 7.63 (d, 1H, *J* = 7.4 Hz, H_{arom}), 7.50 (d, 1H, *J* = 7.1 Hz, H_{arom}), 7.25–7.16 (m, 2H, H_{arom}), 6.87 (d, 2H, *J* = 9.1 Hz, H_{arom}), 3.07 (s, 6H, CH₃); ¹³C NMR (DMSO-d₆, 75 MHz): δ/ppm = 164.4, 152.9, 150.9, 149.4, 145.9, 133.1 (2C), 132.3, 120.3, 119.2, 118.2, 112.3 (2C), 112.1 (2C), 94.2; Anal. Calcd. for C₁₈H₁₆N₄: C, 74.98; H, 5.59; N, 19.43. Found: C, 74.91; H, 5.76; N, 19.38%.

(E)-3-(4-*N,N*-dimethylaminophenyl)-2-(*N*-methylbenzimidazol-2-yl)acrylonitrile 59

Compound **59** was prepared from **19** (0.10 g, 0.6 mmol) and **30** (0.09 g, 0.6 mmol) in absolute ethanol (2 mL) after refluxing for 3.5 h to yield 0.10 g (58%) of red powder; m.p 202–206 °C; ¹H NMR (DMSO-*d*₆, 400 MHz): δ/ppm = 7.97 (s, 1H, H_{arom}), 7.86 (d, 3H, *J* = 9.1 Hz, H_{arom}), 7.60–7.45 (m, 2H, H_{arom}), 6.83 (d, 3H, *J* = 9.1 Hz, H_{arom}), 3.06 (s, 9H, CH₃); ¹³C NMR (DMSO-*d*₆, 101 MHz): δ/ppm = 164.4, 153.4, 150.9, 133.1 (2C), 119.2 (2C), 118.7 (2C), 112.1 (2C), 97.7, 40.0 (3C); Anal. Calcd. for C₁₉H₁₈N₄: C, 75.47; H, 6.00; N, 18.53. Found: C, 75.56; H, 5.94; N, 18.47%.

(E)-3-(4-*N,N*-dimethylaminophenyl)-2-(*N*-phenylbenzimidazol-2-yl)acrylonitrile 60

Compound **60** was prepared from **20** (0.10 g, 0.4 mmol) and **30** (0.06 g, 0.4 mmol) in absolute ethanol (2 mL) after refluxing for 3.5 h to yield 0.11 g (69%) of yellow powder; m.p 206–209 °C; ¹H NMR (DMSO-*d*₆, 300 MHz): δ/ppm = 7.77 (dd, 1H, *J* = 7.0, 1.1 Hz, H_{arom}), 7.73 (d, 3H, *J* = 8.8 Hz, H_{arom}), 7.68–7.56 (m, 5H, H_{arom}), 7.34 (td, 1H, *J* = 7.4, 1.4 Hz, H_{arom}), 7.27 (td, 1H, *J* = 7.9, 1.4 Hz, H_{arom}), 7.17 (dd, 1H, *J* = 7.1, 1.4 Hz, H_{arom}), 6.79 (d, 2H, *J* = 9.1 Hz, H_{arom}), 3.04 (s, 3H, CH₃); ¹³C NMR (DMSO-*d*₆, 75 MHz): δ/ppm = 153.1, 150.6, 148.7, 142.6, 137.4, 136.0, 133.1, 132.4, 130.6, 129.8, 128.0, 124.0, 123.5, 120.0, 119.5, 117.6, 112.1, 110.8, 91.9, 40.0 (2C); Anal. Calcd. for C₂₄H₂₀N₄: C, 79.10; H, 5.53; N, 15.37. Found: C, 79.17; H, 5.47; N, 15.43%.

(E)-3-(4-*N,N*-dimethylaminophenyl)-2-(*N*-hexylbenzimidazol-2-yl)acrylonitrile 61

Compound **61** was prepared from **21** (0.07 g, 0.3 mmol) and **30** (0.04 g, 0.3 mmol) in absolute ethanol (2 mL) after refluxing for 3 h to yield 0.10 g (94%) of brown oil in the form of a mixture of *E*- and *Z*-isomers at a ratio of 61a/61b = 2:1; 61a: ¹H NMR (DMSO-*d*₆, 400 MHz): δ/ppm = 7.99 (s, 1H, H_{arom}), 7.97 (d, 1H, *J* = 9.0 Hz, H_{arom}), 7.67 (d, 1H, *J* = 7.6 Hz, H_{arom}), 7.63 (d, 1H, *J* = 7.9 Hz, H_{arom}), 7.33–7.27 (m, 1H, H_{arom}), 7.27–7.23 (m, 1H, H_{arom}), 6.88 (t, 2H, *J* = 8.7 Hz, H_{arom}), 6.56 (d, 1H, *J* = 9.1 Hz, H_{arom}), 4.43 (t, 2H, *J* = 7.5 Hz, CH₂), 3.08 (s, 6H, CH₃), 1.84–1.76 (m, 2H, CH₂), 1.30–1.20 (m, 6H, CH₂), 0.80 (t, 6H, *J* = 7.0 Hz, CH₃); ¹³C NMR (DMSO-*d*₆, 101 MHz): δ/ppm = 152.8, 151.7, 146.0, 143.1, 135.2, 132.6 (2C), 123.8, 122.8, 120.2, 120.1, 119.9, 112.1 (2C), 111.9, 93.3, 44.2, 31.1, 29.6, 26.1, 22.4, 14.2 (2C); 61b: ¹H NMR (DMSO-*d*₆, 400 MHz): δ/ppm = 7.97 (d, 2H, *J* = 9.0 Hz, H_{arom}), 7.87 (s, 1H, H_{arom}), 7.74 (d, 1H, *J* = 7.8 Hz, H_{arom}), 7.63 (d, 1H, *J* = 7.9 Hz, H_{arom}), 7.38–7.32 (m, 1H, H_{arom}), 7.33–7.27 (m, 1H, H_{arom}), 6.88 (t, 2H, *J* = 8.7 Hz, H_{arom}), 4.03 (t, 2H, *J* = 7.1 Hz, CH₂), 2.92 (s, 6H, CH₃), 1.65–1.59 (m, 2H, CH₂), 1.14–1.08 (m, 6H, CH₂), 0.76 (t, 6H, *J* = 6.7 Hz, CH₃); ¹³C NMR (DMSO-*d*₆, 101 MHz): δ/ppm = 153.1, 151.3, 148.7, 142.6, 136.4, 132.4 (2C), 123.8, 123.2, 120.3, 119.9, 119.4, 111.9 (2C), 111.8, 91.2, 44.4, 31.1, 29.7, 26.2, 22.3, 14.2 (2C); Anal. Calcd. for C₂₄H₂₈N₄: C, 77.38; H, 7.58; N, 15.04. Found: C, 77.41; H, 7.66; N, 15.08%.

(E)-2-(5-cyano-*N*-hexylbenzimidazol-2-yl)-3-(4-*N,N*-dimethylaminophenyl)acrylonitrile 62

Compound **62** was prepared from **25** (0.05 g, 0.2 mmol) and **30** (0.03 g, 0.2 mmol) in absolute ethanol (1.5 mL) after refluxing for 3 h to yield 0.3 g (76%) of orange oil; ¹H NMR (DMSO-*d*₆, 600 MHz): δ/ppm = 8.20 (d, 1H, *J* = 1.0 Hz, H_{arom}), 8.08 (s, 1H, H_{arom}), 7.98 (d, 2H, *J* = 9.1 Hz, H_{arom}), 7.87 (d, 1H, *J* = 9.1 Hz, H_{arom}), 7.69 (dd, 1H, *J* = 8.4, 1.4 Hz, H_{arom}), 6.87 (d, 2H, *J* = 9.1 Hz, H_{arom}), 4.49 (t, 2H, *J* = 7.5 Hz, CH₂), 3.08 (s, 6H, CH₃), 1.81–1.78 (m, 2H, CH₂), 1.26–1.23 (m, 6H, CH₂), 0.80 (t, 3H, *J* = 6.7 Hz, CH₃); ¹³C NMR (DMSO-*d*₆, 151 MHz): δ/ppm = 153.4, 152.4, 151.5, 142.0, 139.3, 133.0 (2C), 126.4, 124.2, 120.2, 120.1, 118.6, 112.8, 112.2 (2C), 105.1, 89.9, 44.8, 31.0, 29.7, 26.0, 22.4, 14.2 (2C); Anal. Calcd. for C₂₅H₂₇N₅: C, 75.54; H, 6.85; N, 17.62. Found: C, 75.61; H, 6.83; N, 17.58%.

(E)-2-(1*H*-benzimidazol-2-yl)-3-(4-*N,N*-diethylaminophenyl)acrylonitrile 63

Compound **63** was prepared from **17** (0.10 g, 0.6 mmol) and **31** (0.11 g, 0.6 mmol) in absolute ethanol (2 mL) after refluxing for 3 h to yield 0.14 g (68%) of orange powder; m.p 151–156 °C; ¹H NMR (DMSO-*d*₆, 300 MHz): δ/ppm = 12.75 (s, 1H, NH_{benz}), 8.10 (s, 1H, H_{arom}), 7.97–7.81 (m, 3H, H_{arom}), 7.53 (bs, 2H, H_{arom}), 7.23–7.17 (m, 1H, H_{arom}), 6.87–6.77

(m, 2H, H_{arom}), 3.47 (q, 4H, $J = 6.4$ Hz, CH_2), 1.15 (t, 6H, $J = 6.7$ Hz, CH_3); ^{13}C NMR (DMSO- d_6 , 151 MHz): $\delta/\text{ppm} = 150.6, 149.5, 145.9, 144.0, 135.3, 133.5, 132.8, 123.2, 122.3, 119.6, 119.0, 118.4$ (2C), 111.8, 111.6, 93.4, 44.4 (2C), 12.9 (2C); Anal. Calcd. for $\text{C}_{20}\text{H}_{20}\text{N}_4$: C, 75.92; H, 6.37; N, 17.71. Found: C, 75.97; H, 6.46; N, 17.76%.

E-(*Z*)-3-(4-*N,N*-diethylaminophenyl)-2-(*N*-isobutylbenzimidazol-2-yl)acrylonitrile **64**

Compound **64** was prepared from **18** (0.10 g, 0.5 mmol) and **31** (0.08 g, 0.5 mmol) in absolute ethanol (2 mL) after refluxing for 3 h to yield 0.10 g (61%) of light red oil in the form of a mixture of *E*- and *Z*-isomers at a ratio of 64a/64b = 2:1; 64a: ^1H NMR (DMSO- d_6 , 600 MHz): $\delta/\text{ppm} = 8.02$ (s, 1H, H_{arom}), 7.95 (d, 2H, $J = 9.1$ Hz, H_{arom}), 7.67–7.63 (m, 2H, H_{arom}), 7.31–7.29 (m, 2H, H_{arom}), 7.24 (td, 1H, $J = 7.6, 1.1$ Hz, H_{arom}), 6.85–6.81 (m, 1H, H_{arom}), 6.52 (d, 1H, $J = 9.2$ Hz, H_{arom}), 4.31 (d, 2H, $J = 7.5$ Hz, CH_2), 3.47 (q, 4H, $J = 7.0$ Hz, CH_2), 2.22–2.09 (m, 1H, CH), 1.15 (t, 6H, $J = 6.9$ Hz, CH_3), 0.83 (d, 6H, $J = 6.7$ Hz, CH_3); ^{13}C NMR (DMSO- d_6 , 151 MHz): $\delta/\text{ppm} = 151.3, 150.9, 148.8, 142.4, 136.9, 133.0$ (2C), 123.1, 122.7, 119.7, 119.3, 119.0, 111.7 (2C), 111.5, 90.6, 51.2, 44.4 (2C), 29.6, 20.1 (2C), 12.9 (2C); 64b: ^1H NMR (DMSO- d_6 , 600 MHz): $\delta/\text{ppm} = 7.79$ (s, 1H, H_{arom}), 7.73 (d, 1H, $J = 7.9$ Hz, H_{arom}), 7.69 (d, 1H, $J = 8.0$ Hz, H_{arom}), 7.35 (td, 1H, $J = 7.5, 1.0$ Hz, H_{arom}), 7.31–7.29 (m, 1H, H_{arom}), 6.85–6.81 (m, 4H, H_{arom}), 3.84 (d, 2H, $J = 7.6$ Hz, CH_2), 3.31 (q, 4H, $J = 6.8$ Hz, CH_2), 2.12–2.08 (m, 1H, CH), 1.02 (t, 6H, $J = 6.9$ Hz, CH_3), 0.79 (d, 6H, $J = 6.6$ Hz, CH_3); ^{13}C NMR (DMSO- d_6 , 151 MHz): $\delta/\text{ppm} = 151.3, 150.5, 146.3, 143.0, 135.5, 132.8$ (2C), 123.7, 122.8, 120.2, 120.1, 119.4, 112.1, 111.6 (2C), 92.6, 51.3, 44.2 (2C), 29.1, 20.2 (2C), 12.8 (2C); Anal. Calcd. for $\text{C}_{24}\text{H}_{28}\text{N}_4$: C, 77.38; H, 7.58; N, 15.04. Found: C, 77.42; H, 7.63; N, 15.10%.

E)-3-(4-*N,N*-diethylaminophenyl)-2-(*N*-methylbenzimidazol-2-yl)acrylonitrile **65**

Compound **65** was prepared from **19** (0.10 g, 0.6 mmol) and **31** (0.10 g, 0.6 mmol) in absolute ethanol (2 mL) after refluxing for 2.5 h to yield 0.12 g (65%) of orange oil; ^1H NMR (DMSO- d_6 , 400 MHz): $\delta/\text{ppm} = 7.95$ (s, 1H, H_{arom}), 7.84 (d, 3H, $J = 9.1$ Hz, H_{arom}), 7.60–7.45 (m, 2H, H_{arom}), 6.80 (d, 3H, $J = 9.1$ Hz, H_{arom}), 3.45 (q, 4H, $J = 7.0$ Hz, H_{arom}), 1.13 (t, 6H, $J = 7.0$ Hz, H_{arom}); ^{13}C NMR (DMSO- d_6 , 101 MHz): $\delta/\text{ppm} = 164.5, 151.2, 150.8$ (2C), 147.5, 133.5 (2C), 133.2, 118.9, 118.6, 111.7 (2C), 111.2, 96.9, 44.4 (2C), 12.9 (3C); Anal. Calcd. for $\text{C}_{21}\text{H}_{22}\text{N}_4$: C, 76.33; H, 6.71; N, 16.96. Found: C, 76.27; H, 6.76; N, 16.88%.

E)-3-(4-*N,N*-diethylaminophenyl)-2-(*N*-phenylbenzimidazol-2-yl)acrylonitrile **66**

Compound **66** was prepared from **20** (0.10 g, 0.4 mmol) and **31** (0.08 g, 0.4 mmol) in absolute ethanol (2.5 mL) after refluxing for 2 h to yield 0.06 g (50%) of red powder; m.p 142–147 °C; ^1H NMR (DMSO- d_6 , 600 MHz): $\delta/\text{ppm} = 7.75$ (d, 1H, $J = 7.9$ Hz, H_{arom}), 7.70 (d, 2H, $J = 9.0$ Hz, H_{arom}), 7.67–7.63 (m, 3H, H_{arom}), 7.61–7.59 (m, 1H, H_{arom}), 7.59–7.56 (m, 2H, H_{arom}), 7.32 (td, 1H, $J = 7.6, 0.9$ Hz, H_{arom}), 7.27 (td, 1H, $J = 8.1, 1.0$ Hz, H_{arom}), 7.15 (d, 1H, $J = 8.0$ Hz, H_{arom}), 6.75 (d, 2H, $J = 9.0$ Hz, H_{arom}), 3.43 (q, 4H, $J = 6.9$ Hz, CH_2), 1.11 (t, 6H, $J = 7.0$ Hz, CH_3); ^{13}C NMR (DMSO- d_6 , 151 MHz): $\delta/\text{ppm} = 150.8, 150.4, 148.9, 142.6, 137.4, 136.1, 132.9$ (2C), 130.6 (2C), 129.7, 128.0 (2C), 124.0, 123.5, 119.5, 119.5, 117.8, 111.7 (2C), 110.7, 91.2, 44.4 (2C), 12.9 (2C); Anal. Calcd. for $\text{C}_{26}\text{H}_{24}\text{N}_4$: C, 79.56; H, 6.16; N, 14.27. Found: C, 79.51; H, 6.26; N, 14.19%.

E-(*Z*)-3-(4-*N,N*-diethylaminophenyl)-2-(*N*-hexylbenzimidazol-2-yl)acrylonitrile **67**

Compound **67** was prepared from **21** (0.07 g, 0.3 mmol) and **31** (0.05 g, 0.3 mmol) in absolute ethanol (2 mL) after refluxing for 3 h to yield 0.10 g (87%) of light red oil in the form of a mixture of *E*- and *Z*-isomers at a ratio of 67a/67b = 2:1; 67a: ^1H NMR (DMSO- d_6 , 400 MHz): $\delta/\text{ppm} = 7.96$ (s, 2H, H_{arom}), 7.69–7.65 (m, 1H, H_{arom}), 7.65–7.61 (m, 1H, H_{arom}), 7.27–7.22 (m, 1H, H_{arom}), 6.87 (d, 1H, $J = 9.1$ Hz, H_{arom}), 6.83 (d, 2H, $J = 9.1$ Hz, H_{arom}), 6.52 (d, 1H, $J = 9.2$ Hz, H_{arom}), 4.43 (t, 2H, $J = 7.4$ Hz, CH_2), 3.48 (q, 4H, $J = 7.0$ Hz, CH_2), 1.84–1.75 (m, 2H, CH_2), 1.30–1.20 (m, 6H, CH_2), 1.15 (t, 6H, $J = 7.0$ Hz, CH_3), 0.80 (t, 3H, $J = 7.0$ Hz, CH_3); ^{13}C NMR (DMSO- d_6 , 151 MHz): $\delta/\text{ppm} = 151.2, 150.9, 148.8, 142.6, 136.4, 133.0$ (2C), 123.2, 122.8, 119.7, 119.3, 118.9, 111.7 (2C), 111.2, 90.4, 44.4 (2C), 31.1, 29.7, 26.1, 22.4, 14.2, 12.9 (2C); 67b: ^1H NMR (DMSO- d_6 , 400 MHz): $\delta/\text{ppm} = 7.94$ (s, 2H, H_{arom}), 7.83 (s, 1H, H_{arom}),

7.74 (d, 1H, $J = 7.4$ Hz, H_{arom}), 7.65–7.61 (m, 1H, H_{arom}), 7.38–7.33 (m, 1H, H_{arom}), 7.32–7.30 (m, 1H, H_{arom}), 7.30–7.27 (m, 2H, H_{arom}), 4.06 (t, 2H, $J = 7.1$ Hz, CH_2), 1.67–1.57 (m, 2H, CH_2), 1.12–1.08 (m, 6H, CH_2), 1.02 (t, 6H, $J = 7.0$ Hz, CH_3), 0.74 (t, 3H, $J = 6.7$ Hz, CH_3); ^{13}C NMR (DMSO- d_6 , 151 MHz): $\delta/\text{ppm} = 151.5, 150.5, 146.1, 143.2, 135.2, 132.8$ (2C), 123.7, 122.8, 120.2, 120.0, 119.5, 111.4 (2C), 111.0, 92.4, 44.2 (2C), 31.2, 29.5, 26.2, 22.3, 14.2, 12.8 (2C); Anal. Calcd. for $\text{C}_{26}\text{H}_{32}\text{N}_4$: C, 77.96; H, 8.05; N, 13.99. Found: C, 77.91; H, 8.16; N, 14.03%.

E-(Z)-2-(6-cyano-*N*-butylbenzimidazol-2-yl)-3-(4-*N,N*-diethylaminophenyl)acrylonitrile **68**

Compound **68** was prepared from **22** (0.10 g, 0.4 mmol) and **31** (0.07 g, 0.4 mmol) in absolute ethanol (2 mL) after refluxing for 3 h to yield 0.10 g (61%) of red oil in the form of a mixture of *E*- and *Z*-isomers at a ratio of 68a/68b = 2:1; 68a: ^1H NMR (DMSO- d_6 , 600 MHz): $\delta/\text{ppm} = 8.20$ (d, 1H, $J = 1.2$ Hz, H_{arom}), 8.13 (s, 1H, H_{arom}), 7.97 (d, 2H, $J = 9.1$ Hz, H_{arom}), 7.68 (dd, 1H, $J = 8.4, 1.4$ Hz, H_{arom}), 6.85–6.81 (m, 2H, H_{arom}), 6.54 (d, 1H, $J = 9.2$ Hz, H_{arom}), 4.39 (d, 2H, $J = 7.6$ Hz, CH_2), 3.48 (q, 4H, $J = 7.0$ Hz, CH_2), 2.18–2.13 (m, 1H, CH), 1.15 (t, 6H, $J = 7.0$ Hz, CH_3), 0.83 (d, 6H, $J = 6.6$ Hz, CH_3);

^{13}C NMR (DMSO- d_6 , 151 MHz): $\delta/\text{ppm} = 152.3, 151.6, 151.2, 141.8, 139.9, 133.5$ (2C), 126.3, 124.1, 120.2, 119.6, 118.7, 113.1, 111.8 (2C), 105.0, 89.4, 51.4, 44.5 (2C), 29.7, 19.9 (2C), 12.9 (2C); 68b: ^1H NMR (DMSO- d_6 , 600 MHz): $\delta/\text{ppm} = 8.33$ (d, 1H, $J = 1.0$ Hz, H_{arom}), 7.95 (d, 1H, $J = 8.6$ Hz, H_{arom}), 7.90 (d, 2H, $J = 8.4$ Hz, H_{arom}), 7.86 (s, 1H, H_{arom}), 7.76 (dd, 1H, $J = 8.5, 1.5$ Hz, H_{arom}), 6.85–6.81 (m, 2H, H_{arom}), 3.91 (d, 2H, $J = 7.6$ Hz, CH_2), 3.32 (q, 4H, $J = 6.8$ Hz, CH_2), 2.10–2.05 (m, 1H, CH), 1.02 (t, 6H, $J = 7.0$ Hz, CH_3), 0.79 (d, 6H, $J = 6.6$ Hz, CH_3); ^{13}C NMR (DMSO- d_6 , 151 MHz): $\delta/\text{ppm} = 152.1, 150.7, 149.3, 142.4, 138.4, 132.9$ (2C), 127.0, 125.3, 120.1, 119.8, 119.1, 113.8, 111.6 (2C), 105.3, 91.2, 51.5, 44.2 (2C), 29.2, 20.0 (2C), 12.8 (2C); Anal. Calcd. for $\text{C}_{25}\text{H}_{27}\text{N}_5$: C, 75.54; H, 6.85; N, 17.62. Found: C, 75.50; H, 6.89; N, 17.57%.

E)-2-(6-cyano-*N*-methylbenzimidazol-2-yl)-3-(4-*N,N*-diethylaminophenyl)acrylonitrile **69**

Compound **69** was prepared from **23** (0.10 g, 0.5 mmol) and **31** (0.09 g, 0.5 mmol) in absolute ethanol (2 mL) after refluxing for 2.5 h to yield 0.15 g (84%) of red powder; m.p 164–169 °C; ^1H NMR (DMSO- d_6 , 300 MHz): $\delta/\text{ppm} = 8.18$ (s, 1H, H_{arom}), 7.99 (d, 2H, $J = 4.7$ Hz, H_{arom}), 7.95 (s, 1H, H_{arom}), 7.82 (d, 1H, $J = 8.4$ Hz, H_{arom}), 7.68 (dd, 1H, $J = 8.4, 1.4$ Hz, H_{arom}), 6.84 (d, 2H, $J = 9.1$ Hz, H_{arom}), 4.00 (s, 3H, CH_3), 3.48 (q, 4H, $J = 7.0$ Hz, H_{arom}), 1.15 (t, 6H, $J = 7.0$ Hz, H_{arom}); ^{13}C NMR (DMSO- d_6 , 151 MHz): $\delta/\text{ppm} = 152.3, 151.7, 151.1, 142.0, 140.0, 133.4$ (2C), 126.3, 124.0, 120.3, 119.6, 118.7, 112.5, 111.7 (2C), 104.9, 89.8, 44.5 (2C), 32.5, 13.0 (2C); Anal. Calcd. for $\text{C}_{22}\text{H}_{21}\text{N}_5$: C, 74.34; H, 5.96; N, 19.70. Found: C, 74.28; H, 5.86; N, 19.78%.

E)-2-(6-cyano-*N*-phenylbenzimidazol-2-yl)-3-(4-*N,N*-diethylaminophenyl)acrylonitrile **70**

Compound **70** was prepared from **24** (0.10 g, 0.4 mmol) and **31** (0.07 g, 0.4 mmol) in absolute ethanol (2 mL) after refluxing for 2 h to yield 0.14 g (86%) of red powder; m.p 210–214 °C; ^1H NMR (DMSO- d_6 , 300 MHz): $\delta/\text{ppm} = 8.31$ (d, 1H, $J = 0.8$ Hz, H_{arom}), 7.74 (s, 2H, H_{arom}), 7.70 (s, 1H, H_{arom}), 7.69–7.57 (m, 6H, H_{arom}), 7.29 (d, 1H, $J = 8.5$ Hz, H_{arom}), 6.77 (d, 2H, $J = 9.1$ Hz, H_{arom}), 3.45 (q, 4H, $J = 6.9$ Hz, CH_2), 1.13 (t, 6H, $J = 7.0$ Hz, CH_3); ^{13}C NMR (DMSO- d_6 , 75 MHz): $\delta/\text{ppm} = 151.7, 151.5, 151.2, 142.2, 140.3, 135.3, 133.2$ (2C), 130.7 (2C), 130.3, 128.1 (2C), 127.2, 124.2, 120.1, 119.3, 117.4, 112.2, 111.8, 105.7, 90.1, 44.5 (2C), 12.7 (2C); Anal. Calcd. for $\text{C}_{27}\text{H}_{23}\text{N}_5$: C, 77.67; H, 5.55; N, 16.77. Found: C, 77.61; H, 5.66; N, 16.73%.

E)-2-(6-cyano-*N*-hexylbenzimidazol-2-yl)-3-(4-*N,N*-diethylaminophenyl)acrylonitrile **71**

Compound **71** was prepared from **25** (0.05 g, 0.2 mmol) and **31** (0.03 g, 0.2 mmol) in absolute ethanol (1.5 mL) after refluxing for 3 h to yield 0.03 g (40%) of orange powder; m.p 118–122 °C; ^1H NMR (DMSO- d_6 , 400 MHz): $\delta/\text{ppm} = 8.19$ (d, 1H, $J = 1.0$ Hz, H_{arom}), 8.05 (s, 1H, H_{arom}), 7.97 (d, 2H, $J = 9.1$ Hz, H_{arom}), 7.87 (d, 1H, $J = 8.5$ Hz, H_{arom}), 7.69 (dd, 1H, $J = 8.4, 1.4$ Hz, H_{arom}), 6.84 (d, 2H, $J = 9.2$ Hz, H_{arom}), 4.49 (t, 2H, $J = 7.4$ Hz,

CH₂), 3.49 (q, 4H, *J* = 6.9 Hz, CH₂), 1.84–1.75 (m, 2H, CH₂), 1.30–1.20 (m, 6H, CH₂), 1.15 (t, 6H, *J* = 6.7 Hz, CH₃), 0.80 (t, 3H, *J* = 6.7 Hz, CH₃); ¹³C NMR (DMSO-d₆, 151 MHz): δ/ppm = 152.2, 151.6, 151.2, 142.0, 139.4, 133.5 (2C), 126.4, 124.1, 120.3, 119.5, 118.7, 112.8, 111.8 (2C), 105.0, 89.2, 44.8, 44.5 (2C), 31.0, 29.7, 26.0, 22.4, 14.2, 12.9 (2C); Anal. Calcd. for C₂₇H₃₁N₅: C, 76.20; H, 7.34; N, 16.46. Found: C, 76.23; H, 7.28; N, 16.38%.

3.2. Biology

3.2.1. Cell Culture and Reference Compounds

Capan-1, HCT-116, NCI-H460, LN-229, HL-60, K-562, and Z-138 cancer cell lines were acquired from the American Type Culture Collection (ATCC, Manassas, VA, USA), while the DND-41 cell line was purchased from Deutsche Sammlung von Mikroorganismen und Zellkulturen (DSMZ Leibniz-Institut, Braunschweig, Germany). Culture media were purchased from Gibco Life Technologies, Carlsbad, CA, USA, and supplemented with 10% fetal bovine serum (HyClone, Laboratories Inc., Logan, UT, USA). Docetaxel, which was used as a reference inhibitor, was purchased from Selleckchem (Munich, Germany), while combretastatin A4 (CA4) was obtained from Sigma-Aldrich (St. Louis, MO, USA). Stock solutions were prepared in DMSO.

3.2.2. Proliferation Assays

Adherent cell lines LN-229, HCT-116, NCI-H460, and Capan-1 cells were seeded at a density range of 500 and 1500 cells per well in 384-well tissue culture plates (Bio-One, Kremsmünster, Austria Greiner). After overnight incubation, cells were treated with four different concentrations of the test compounds, ranging from 100 to 0.8 μM. Suspension cell lines HL-60, K-562, Z-138, and DND-41 were seeded at densities ranging from 2500 to 5500 cells per well in 384-well culture plates containing the test compounds at the same concentration points. The plates were incubated and monitored at 37 °C for 72 h in an IncuCyte® (city, state, country Sartorius, Göttingen, Germany) for real-time imaging of cell proliferation. Brightfield images were taken every 3 h, with one field imaged per well under 10× magnification. Cell growth was then quantified based on the percent cellular confluence as analyzed by the IncuCyte® image analysis software and used to calculate IC₅₀ values via logarithmic interpolation. Compounds were tested in two independent experiments.

3.2.3. Apoptosis Induction in Normal PBMC

Buffy coat preparations from healthy donors were obtained from the Blood Transfusion Center in Leuven, Belgium. Peripheral blood mononuclear cells (PBMC) were isolated by density gradient centrifugation over Lymphoprep (d = 1.077 g mL⁻¹) (Nycomed, Oslo, Norway) and cultured in cell culture medium (DMEM/F12, Gibco Life Technologies, USA) containing 8% FBS. PBMC were seeded at 28,000 cells per well in 384-well, black-walled, clear-bottomed tissue culture plates containing the test compounds at six different concentrations ranging from 20 to 0.006 μM. Propidium iodide was added at a final concentration of 1 μg mL⁻¹ and IncuCyte® Caspase 3/7 Green Reagent was added as recommended by the supplier. The plates were incubated and monitored at 37 °C for 72 h in the IncuCyte®. Images were taken every 3 h in the brightfield and the green and red fluorescence channels, with one field imaged per well under 10x magnification. Quantification of the fluorescent signal after 24 h in both channels using the IncuCyte® image analysis software allowed the percentages of live, dead, and apoptotic cells to be calculated. All compounds were tested in two independent experiments and PBMC originated from two different healthy donors.

3.2.4. Tubulin Polymerization Assay

In vitro tubulin polymerization was carried out using the fluorescence-based tubulin polymerization assay (BK011P, Cytoskeleton, Denver, CO, USA), as described by the manufacturer. Briefly, half-area 96-well plates were warmed to 37 °C 10 min prior to

assay start. Test systems and reference compounds were prepared at 10× stock solutions and added in 5 µL in duplicate wells. Ice-cold tubulin polymerization buffer (2 mg mL⁻¹ tubulin in 80 nM Pipes, 2 mM MgCl₂, 0.5 mM EGTA, pH 6.9, and 10 µM fluorescent reporter + 15% glycerol + 1 mM GTP) was added into each well, followed by reading with a Tecan Spark fluorimeter in kinetic mode, with 61 cycles of 1 reading per minute at 37 °C, 4 reads per well (Ex. 350 nm and Em. 435 nm).

3.3. Computational Details

The structures of all ligands were optimized with Gaussian 16 [30] using the M06-2X DFT functional with the 6-31+G(d) basis set, and these were considered as neutral systems based on the analysis of the pK_a values for similarly substituted benzimidazoles [31]. To account for the effect of the solution, during the geometry optimization we included the implicit SMD polarizable continuum model [32] corresponding to pure water or ethanol, in line with experimental conditions, as utilized in many of our studies concerning various aspects of biomolecular systems [27,33–35]. This approach identified the most stable conformations of all ligands, considering both *E*- and *Z*-isomers around the central C=C double bond. The structure of colchicine was extracted from the non-polymerized colchicine-tubulin crystal structure (5EYP.pdb) [36] and employed as such. This structure was selected since it has the highest resolution among tubulin structures pertaining to the colchicine binding site (1.90 Å) [37], but also to place the current results in line with our earlier reports [27] and other literature recommendations [38–40]. Tubulin's β-subunit was pulled out from the complex and prepared for the docking analysis, while both α- and β-subunits were used for the visualization of the results, with the UCSF Chimera program used for both (version 1.12) [41]. The molecular docking studies were performed with Swiss-Dock [42], a web server used for docking of small molecules on target proteins based on the EADock DSS engine, taking into account the entire protein surface as a potential binding site for the investigated ligands.

For the MD simulations, the investigated ligands were parameterized through RESP charges at the HF/6-31G(d) level to be consistent with the used GAFF force field. The identified binding poses for both *E*- and *Z*-isomers of **64** were solvated in a 10 Å octahedral box, which allowed for around 12,380 water molecules, and were neutralized by 12 Na⁺ cations. These were submitted to geometry optimization in AMBER 16 [43] with periodic boundary conditions in all directions. The optimized systems were gradually heated from 0 to 300 K and equilibrated during 30 ps using NVT conditions, followed by productive and unconstrained MD simulations of 300 ns by employing a time step of 2 fs at a constant pressure (1 atm) and temperature (300 K), with the latter held constant using a Langevin thermostat with a collision frequency of 1 ps⁻¹. The non-bonded interactions were truncated at 11.0 Å, all in line with our earlier reports on similar systems [27,33–35]. The corresponding binding free energies were calculated on 3000 structures from the last 30 ns of simulations using the MM-GBSA protocol [44,45] available in AmberTools16 [43], then decomposed into specific residue contributions on a per-residue basis according to the established procedure [46,47].

4. Conclusions

We presented the design, synthesis, computational analysis, and antiproliferative evaluation of novel benzimidazole-derived acrylonitriles prepared by the cyclocondensation of the corresponding *N*-substituted 2-(cyanomethyl)-benzimidazoles with benzaldehyde and 2-methoxy, 2,4-dimethoxy, 3,4,5-trimethoxy, 4-*N,N*-dimethylamino, and 4-*N,N*-diethylamino-substituted benzaldehydes. The N-atom of benzimidazole core was substituted with methyl, *i*-butyl, phenyl, or *n*-hexyl substituents, while some of the derivatives additionally showed a cyano group at the benzimidazole ring.

All newly prepared derivatives were tested on eight human cancer cell lines. The majority of the compounds displayed weak to moderate antiproliferative activity without significant selectivity among the tested cell lines.

The most active derivatives were proven to be compounds **50**, **64**, **68**, and **69** substituted with the 2,4-dimethoxyphenyl and 4-*N,N*-diethylaminophenyl rings bearing the phenyl, *i*-butyl, and methyl substituents at the N-atom of the benzimidazole core with (**50**, **68**, and **69**) and without (**64**) the cyano group. These compounds showed selective inhibitory activity (IC₅₀ 1.7–3.6 μM) against all tested hematological tumor cell lines, namely acute lymphoblastic (DND-41) and myeloid leukemia (HL-60), chronic myeloid leukemia (K-562), and non-Hodgkin lymphoma (Z-138). The evaluation of normal PBMC showed that the antiproliferative activity of compounds **50**, **64**, **68**, and **69** was selective towards cancer cells.

It remains a challenge to demonstrate acceptable pharmacokinetic and neuropathic properties, as well as the suitable antitumor effects of the identified lead compounds *in vivo*, which is planned for the next phase of this research.

Further mechanism of action studies revealed that these derivatives exert their anti-tumor activity by inhibiting the polymerization of tubulin, while computational analysis confirmed **64** as the most potent ligand for the colchicine binding site in tubulin, where it benefits from the S–H···N(Et₂) interaction with Cys241, N–H···π interactions with Lys254, N–H···N hydrogen bonds with Asn258, and N–H···N≡C hydrogen bonds with Lys352, while its bulky *N*-*i*-butyl group allows deeper entrance into the hydrophobic pocket within the tubulin's β-subunit, predominantly consisting of Leu255, Leu248, Met259, Ala354, and Ile378 residues.

Supplementary Materials: The following are available online at <https://www.mdpi.com/article/10.3390/ph14101052/s1>. Figures S1–S119: NMR spectra of novel compounds. Figures S120–S128: Computational chemistry.

Author Contributions: Design, synthesis, spectroscopic characterization, and methodology, A.B. and M.H. Computational chemistry and analysis, L.H. and R.V. Biological activity and tubulin polymerization inhibition, L.P., E.V. and D.D. Writing of the manuscript and interpretation of the results, A.B., L.H., L.P., D.D., R.V. and M.H. All authors read and approved the final version of the manuscript.

Funding: We greatly appreciate the financial support of the Croatian Science Foundation under the projects 4379 entitled Exploring the Antioxidative Potential of the Benzazole Scaffold in the Design of Novel Antitumor Agents.

Institutional Review Board Statement: Not applicable.

Informed Consent Statement: Not applicable.

Data Availability Statement: Data is contained within the article.

Conflicts of Interest: The authors declare no conflict of interest.

References

1. Jordan, M.A.; Wilson, L. Microtubules as a target for anticancer drugs. *Nat. Rev. Cancer* **2004**, *4*, 253–265. [[CrossRef](#)]
2. Seligmann, J.; Twelves, C. Tubulin: An example of targeted chemotherapy. *Future Med. Chem.* **2013**, *5*, 339–352. [[CrossRef](#)]
3. Vindya, N.G.; Sharma, N.; Yadav, M.; Ethiraj, K.R. Tubulins—The target for anticancer therapy. *Curr. Top. Med. Chem.* **2015**, *15*, 73–82. [[CrossRef](#)]
4. Kingston, D.G.I. Tubulin–Interactive natural products as anticancer agents. *J. Nat. Prod.* **2009**, *72*, 507–515. [[CrossRef](#)] [[PubMed](#)]
5. Dumontet, C.; Jordan, M.A. Microtubule-binding agents: A dynamic field of cancer therapeutics. *Nat. Rev. Drug Discov.* **2010**, *9*, 790–803. [[CrossRef](#)] [[PubMed](#)]
6. Sengupta, S.; Thomas, S.A. Drug target interaction of tubulin-binding drugs in cancer therapy. *Expert Rev. Anticancer Ther.* **2006**, *6*, 1433–1447. [[CrossRef](#)] [[PubMed](#)]
7. Li, W.; Sun, H.; Xu, S.; Zhu, Z.; Xu, J. Tubulin inhibitors targeting the colchicine binding site: A perspective of privileged structures. *Future Med. Chem.* **2017**, *9*, 1765–1794. [[CrossRef](#)] [[PubMed](#)]
8. Xi, J.; Zhu, X.; Feng, Y.; Huang, N.; Luo, G.; Mao, Y.; Han, X.; Tian, W.; Wang, G.; Han, X.; et al. Development of a novel class of tubulin inhibitors with promising anticancer activities. *Mol. Cancer Res.* **2013**, *11*, 856–864. [[CrossRef](#)] [[PubMed](#)]
9. Mandhare, A.; Banerjee, P. Therapeutic use of colchicine and its derivatives: A patent review. *Expert Opin. Ther. Pat.* **2016**, *29*, 1–18. [[CrossRef](#)] [[PubMed](#)]

10. Fu, D.J.; Liu, S.M.; Li, F.H.; Yang, J.J.; Li, J. Antiproliferative benzothiazoles incorporating a trimethoxyphenyl scaffold as novel colchicine site tubulin polymerisation inhibitors. *J. Enzym. Inhib. Med. Chem.* **2020**, *35*, 1050–1059. [[CrossRef](#)]
11. Zhou, J.; Giannakakou, P. Targeting microtubules for cancer chemotherapy. *Curr. Med. Chem. Anticancer Agents* **2005**, *5*, 65–71. [[CrossRef](#)]
12. Kaur, R.; Kaur, G.; Kaur Gill, R.; Soni, R.; Bariwal, J. Recent developments in tubulin polymerization inhibitors: An overview. *Eur. J. Med. Chem.* **2014**, *8*, 89–124. [[CrossRef](#)]
13. Hranjec, M.; Kralj, M.; Piantanida, I.; Sedić, M.; Šuman, L.; Pavelić, K.; Karminski-Zamola, G. Novel cyano- and amidino-substituted derivatives of styryl-2-benzimidazoles and benzimidazo[1,2-a]quinolines. Synthesis, photochemical synthesis, DNA binding and antitumor evaluation, Part 3. *J. Med. Chem.* **2007**, *50*, 5696–5711. [[CrossRef](#)]
14. Perin, N.; Nhili, R.; Cindrić, M.; Bertoša, B.; Vušak, D.; Martin-Kleiner, I.; Laine, W.; Karminski-Zamola, G.; Kralj, M.; David-Cordonnier, M.H.; et al. Amino substituted benzimidazo[1,2-a]quinolines: Antiproliferative potency, 3D QSAR study and DNA binding properties. *Eur. J. Med. Chem.* **2016**, *122*, 530–545. [[CrossRef](#)]
15. Yellol, J.; Pérez, S.A.; Buceta, A.; Yellol, G.; Donaire, A.; Szumlas, P.; Bednarski, P.J.; Makhloufi, G.; Janiak, C.; Espinosa, A.; et al. Novel C,N-cyclometalated benzimidazole ruthenium(II) and iridium(III) complexes as antitumor and antiangiogenic agents: A structure-activity relationship study. *J. Med. Chem.* **2015**, *58*, 7310–7327. [[CrossRef](#)]
16. Munuganti, R.S.N.; Leblanc, E.; Axerio-Cilies, P.; Labriere, C.; Frewin, K.; Singh, K.; Hassona, M.D.H.; Lack, N.A.; Li, H.; Ban, F.; et al. Targeting the binding function 3 (BF3) site of the androgen receptor through virtual screening. 2. development of 2-((2-phenoxyethyl) thio)-1H-benzimidazole derivatives. *J. Med. Chem.* **2013**, *56*, 1136–1148. [[CrossRef](#)] [[PubMed](#)]
17. Snow, R.J.; Abeywardane, A.; Campbell, S.; Lord, J.; Kashem, M.A.; Khine, H.H.; King, J.; Kowalski, J.A.; Pullen, S.S.; Roma, T.; et al. Hit-to-lead studies on benzimidazole inhibitors of ITK: Discovery of a novel class of kinase inhibitors. *Bioorg. Med. Chem.* **2007**, *17*, 3660–3665. [[CrossRef](#)] [[PubMed](#)]
18. Garuti, L.; Roberti, M.; Bottegoni, G. Benzimidazole derivatives as kinase inhibitors. *Curr. Med. Chem.* **2014**, *21*, 2284–2298. [[CrossRef](#)] [[PubMed](#)]
19. Shi, W.; Siemann, D.W. Preclinical studies of the novel vascular disrupting agent MN-029. *Anticancer Res.* **2005**, *25*, 3899–3904. [[PubMed](#)]
20. Kamal, A.; Reddy, T.S.; Vishnuvardhan, M.V.P.S.; Nimbarte, V.D.; Rao, A.V.S.; Srinivasulu, V.; Shankaraiah, N. Synthesis of 2-aryl-1,2,4-oxadiazolo-benzimidazoles: Tubulin polymerization inhibitors and apoptosis inducing agents. *Bioorg. Med. Chem.* **2015**, *23*, 4608–4623. [[CrossRef](#)]
21. Sanna, P.; Carta, A.; Rahbar Nikookar, M.E. Synthesis and antitubercular activity of 3-aryl substituted-2-(1H(2H)benzotriazol-1(2)-yl)acrylonitriles. *Eur. J. Med. Chem.* **2000**, *35*, 535–543. [[CrossRef](#)]
22. Carta, A.; Sanna, P.; Palomba, M.; Vargiu, L.; La Colla, M.; Loddo, R. Synthesis and antiproliferative activity of 3-aryl-2-(1H-benzotriazol-1-yl)acrylonitriles. Part III. *Eur. J. Med. Chem.* **2002**, *37*, 891–900. [[CrossRef](#)]
23. Vasquez, R.J.; Howell, B.; Yvon, A.M.; Wadsworth, P.; Cassimeris, L. Nanomolar concentrations of nocodazole alter microtubule dynamic instability in vivo and in vitro. *Mol. Biol. Cell* **1997**, *8*, 973–985. [[CrossRef](#)] [[PubMed](#)]
24. Hasanpourghadi, M.; Karthikeyan, C.; Pandurangan, A.K.; Looi, C.Y.; Trivedi, P.; Kobayashi, K.; Tanaka, K.; Wong, W.F.; Mustafa, M.R. Targeting of tubulin polymerization and induction of mitotic blockage by Methyl 2-(5-fluoro-2-hydroxyphenyl)-1H-benzo[d]imidazole-5-carboxylate (MBIC) in human cervical cancer HeLa cell. *J. Exp. Clin. Cancer Res.* **2016**, *35*, 58. [[CrossRef](#)]
25. Wang, W.; Kong, D.; Cheng, H.; Tan, L.; Zhang, Z.; Zhuang, X.; Long, H.; Zhou, Y.; Xu, Y.; Yang, X.; et al. New benzimidazole-2-urea derivatives as tubulin inhibitors. *Bioorg. Med. Chem. Lett.* **2014**, *24*, 4250–4253. [[CrossRef](#)]
26. Miao, T.T.; Tao, X.B.; Li, D.D.; Chen, H.; Jin, X.; Geng, Y.; Wang, S.F.; Gu, W. Synthesis and biological evaluation of 2-arylbenzimidazole derivatives of dehydroabietic acid as novel tubulin polymerization inhibitors. *RSC Adv.* **2018**, *8*, 17511–17526. [[CrossRef](#)]
27. Perin, N.; Hok, L.; Beč, A.; Persoons, L.; Vanstreels, E.; Daelemans, D.; Vianello, R.; Hranjec, M. N-substituted benzimidazole acrylonitriles as in vitro tubulin polymerization inhibitors: Synthesis, biological activity and computational analysis. *Eur. J. Med. Chem.* **2021**, *211*, 113003. [[CrossRef](#)] [[PubMed](#)]
28. Silva-García, E.M.; Cerda-García-Rojas, C.M.; del Río, R.E.; Joseph-Nathan, P. Parvifoline derivatives as tubulin polymerization inhibitors. *J. Nat. Prod.* **2019**, *82*, 840–849. [[CrossRef](#)] [[PubMed](#)]
29. Wilson, L.; Meza, I. The mechanism of action of colchicine. *J. Cell Biol.* **1973**, *58*, 709–719. [[CrossRef](#)] [[PubMed](#)]
30. Frisch, M.J.; Trucks, G.W.; Schlegel, H.B.; Scuseria, G.E.; Robb, M.A.; Cheeseman, J.R.; Scalmani, G.; Barone, V.; Petersson, G.A.; Nakatsuji, H.; et al. *Gaussian 16, Revision C.01*; Gaussian Inc.: Wallingford, CT, USA, 2016.
31. Tshepelevitsh, S.; Kütt, A.; Lökov, M.; Kaljurand, I.; Saame, J.; Heering, A.; Pliieger, P.; Vianello, R.; Leito, I. On the Basicity of Organic Bases in Different Media. *Eur. J. Org. Chem.* **2019**, *2019*, 6735–6748. [[CrossRef](#)]
32. Marenich, A.V.; Cramer, C.J.; Truhlar, D.G. Universal solvation model based on solute electron density and on a continuum model of the solvent defined by the bulk dielectric constant and atomic surface tensions. *J. Phys. Chem. B* **2009**, *113*, 6378–6396. [[CrossRef](#)] [[PubMed](#)]
33. Hok, L.; Mavri, J.; Vianello, R. The effect of deuteration on the H₂ receptor histamine binding profile: A computational insight into modified hydrogen bonding interactions. *Molecules* **2020**, *25*, 6017. [[CrossRef](#)] [[PubMed](#)]

34. Tandarić, T.; Vianello, R. Computational insight into the mechanism of the irreversible inhibition of monoamine oxidase enzymes by the anti-parkinsonian propargylamine inhibitors rasagiline and selegiline. *ACS Chem. Neurosci.* **2019**, *103*, 3532–3542. [[CrossRef](#)] [[PubMed](#)]
35. Maršavelski, A.; Vianello, R. What a difference a methyl group makes—the selectivity of monoamine oxidase B towards histamine and *N*-methylhistamine. *Chem. Eur. J.* **2017**, *23*, 2915–2925. [[CrossRef](#)]
36. Ahmad, S.; Pecqueur, L.; Dreier, B.; Hamdane, D.; Aumont-Nicaise, M.; Pluckthun, A.; Knossow, M.; Gigant, B. Destabilizing an interacting motif strengthens the association of a designed ankyrin repeat protein with tubulin. *Sci. Rep.* **2016**, *6*, 28922. [[CrossRef](#)]
37. Steinmetz, M.O.; Prota, A.E. Microtubule-targeting agents: Strategies to hijack the cytoskeleton. *Trends Cell Biol.* **2018**, *28*, 776–792. [[CrossRef](#)]
38. Halawa, A.H.; Elaasser, M.M.; El Kerdawy, A.M.; Abd El-Hady, A.M.A.I.; Emam, H.A.; El-Agrody, A.M. Anticancer activities, molecular docking and structure–activity relationship of novel synthesized 4*H*-chromene, and 5*H*-chromeno[2,3-*d*]pyrimidine candidates. *Med. Chem. Res.* **2017**, *26*, 2624–2638. [[CrossRef](#)]
39. Traversi, G.; Staid, D.S.; Fiore, M.; Percario, Z.; Trisciuglio, D.; Antonioletti, R.; Morea, V.; Degrassi, F.; Cozzi, R. A novel resveratrol derivative induces mitotic arrest, centrosome fragmentation and cancer cell death by inhibiting γ -tubulin. *Cell Div.* **2019**, *14*, 3. [[CrossRef](#)]
40. Wang, W.; Cantos-Fernandes, S.; Lv, Y.; Kuerban, H.; Ahmad, S.; Wang, C.; Gigant, B. Insight into microtubule disassembly by kinesin-13s from the structure of Kif2C bound to tubulin. *Nat. Commun.* **2017**, *8*, 70. [[CrossRef](#)]
41. Pettersen, E.F.; Goddard, T.D.; Huang, C.C.; Couch, G.S.; Greenblatt, D.M.; Meng, E.C.; Ferrin, T.E. UCSF Chimera-A Visualization System for Exploratory Research and Analysis. *J. Comput. Chem.* **2004**, *13*, 1605–1612. [[CrossRef](#)]
42. Grosdidier, A.; Zoete, V.; Michielin, O. SwissDock, a protein-small molecule docking web service based on EADock DSS. *Nucleic Acids Res.* **2011**, *39*, W270–W277. [[CrossRef](#)] [[PubMed](#)]
43. Case, D.A.; Betz, R.M.; Cerutti, D.S.; Cheatham, T.E., III; Darden, T.A.; Duke, R.E.; Giese, T.J.; Gohlke, H.; Goetz, A.W.; Homeyer, N.; et al. *AMBER 2016*; University of California: San Francisco, CA, USA, 2016.
44. Genheden, S.; Ryde, U. The MM/PBSA and MM/GBSA methods to estimate ligand-binding affinities. *Expert Opin. Drug Discov.* **2015**, *10*, 449–461. [[CrossRef](#)] [[PubMed](#)]
45. Hou, T.; Wang, J.; Li, Y.; Wang, W. Assessing the Performance of the MM/PBSA and MM/GBSA Methods. 1. The Accuracy of Binding Free Energy Calculations Based on Molecular Dynamics Simulations. *J. Chem. Inf. Model.* **2011**, *51*, 69–82. [[CrossRef](#)] [[PubMed](#)]
46. Gohlke, H.; Kiel, C.; Case, D.A. Insights into Protein-Protein Binding by Binding Free Energy Calculation and Free Energy Decomposition for the Ras-Raf and Ras-RalGDS Complexes. *J. Mol. Biol.* **2003**, *330*, 891–913. [[CrossRef](#)]
47. Rastelli, G.; Del Rio, A.; Degliesposti, G.; Sgobba, M. Fast and accurate predictions of binding free energies using MM-PBSA and MM-GBSA. *J. Comput. Chem.* **2010**, *31*, 797–810. [[CrossRef](#)] [[PubMed](#)]